U.PORTO

MASTER´S DEGREE
NEUROBIOLOGY

High-Definition Transcranial Direct Current Stimulation Over the Primary Visual Cortex in Healthy Adults: A Multimodal Visual and Cortical Approach

Rúben João Moreira da Cunha Magalhães

M

2025

U.PORTO
FM UP FACULDADE DE MEDICINA UNIVERSIDADE DO PORTO

Master's Dissertation presented to the Faculty of Medicine of the University of Porto in fulfillment of the requirements for the master's degree in Neurobiology

High-Definition Transcranial Direct Current Stimulation Over the Primary Visual Cortex in Healthy Adults: A Multimodal Visual and Cortical Approach

Rúben João Moreira da Cunha Magalhães

Supervisor

Prof. Catarina Mateus, PhD

Co-supervisors

Prof. Nuno Rocha, PhD

Prof. Carlos Reguenga, PhD

Work conducted at the Center for Translational Health and Medical Biotechnology Research within the Health Research Network (RISE-HEALTH@TBIO), a research center at the School of Health, Polytechnic University of Porto

RISE HEALTH
Health Research and Innovation
From Lab to Community and back to Lab

Center for Translational Health and Medical Biotechnology Research

P.PORTO

ESCOLA SUPERIOR DE SAÚDE

Porto, 2025

Acknowledgments

Ao concluir esta etapa tão significativa do meu percurso académico, não posso deixar de expressar a minha profunda gratidão a todas as pessoas que, de uma forma ou de outra, contribuíram para a realização deste trabalho.

Em primeiro lugar, quero agradecer a todas as pessoas que me acolheram e apoiaram ao longo destes anos no TBIO, pela partilha de conhecimento, pela disponibilidade e pelo ambiente de colaboração que tanto enriqueceram a minha experiência. Um agradecimento muito especial à Inês, pela ajuda, amizade, paciência e companheirismo inestimáveis.

À minha orientadora, Professora Catarina Mateus, quero expressar a minha mais profunda admiração e gratidão. Foi um verdadeiro privilégio poder contar com a sua orientação ao longo deste percurso. A sua dedicação, o seu rigor científico e a forma como partilha o seu conhecimento são para mim uma inspiração constante. A Professora Catarina não foi apenas uma orientadora, mas também um exemplo de excelência académica e humana, e será sempre uma referência no meu caminho profissional e pessoal.

Quero também deixar uma palavra muito especial à minha mãe. Embora apenas esteja presente em coração, espero que esteja orgulhosa do caminho que tenho feito. Este trabalho é por mim, mas também por ela. Sem o amor incondicional e as oportunidades que me proporcionou, eu não teria chegado até aqui. Tudo o que sou devo, em grande parte, à mulher extraordinária que ela foi.

Agradeço de coração às minhas irmãs, Bia e Lili, pelo amor, pela força e por estarem sempre presentes, mesmo nos momentos mais difíceis. Ao meu pai, pelo apoio constante, e ao meu primo Zé Pedro, por nos ter sempre como prioridade e ser incansável sempre que preciso.

Sem dúvida que, nos próximos passos que der, seja na vida académica, profissional ou pessoal, que posso continuar a contar convosco. A todos, um sincero obrigado!

Resumo

Introdução: A estimulação transcraniana por corrente contínua de alta-definição (HD-tDCS) é uma técnica de estimulação cerebral não invasiva que utiliza correntes elétricas focalizadas para modular a atividade neural em regiões específicas do cérebro. Através da colocação de elétrodos ânodo e cátodo, de forma a induzir um fluxo de corrente unidirecional, um número crescente de evidências sugere que a estimulação elétrica do córtex visual primário (V1) pode melhorar as funções visuais. Ao direcionar a estimulação para V1, essencial para o processamento visual cortical, o objetivo é avaliar os efeitos visuais e corticais da HD-tDCS anódica numa amostra de adultos saudáveis. O estudo dos efeitos imediatos e repetidos da HD-tDCS na excitabilidade do V1 tem como finalidade esclarecer os mecanismos envolvidos e explorar as potenciais aplicações clínicas em perturbações visuais e do neurodesenvolvimento.

Objetivos: Este estudo teve como objetivo investigar o impacto da HD-tDCS anódica sobre o córtex visual primário na sensibilidade ao contraste (CS) em adultos saudáveis. Foram também avaliados os efeitos da HD-tDCS anódica na melhor acuidade visual corrigida (BCVA), na amplitude e tempo de culminação da onda P100 dos potenciais evocados visuais (VEP), na amplitude e tempo de culminação das ondas P50 e N95 da eletrorretinografia *pattern* (PERG), bem como na estrutura retiniana. Os efeitos da HD-tDCS foram avaliados através da comparação de medições pré-estimulação com os efeitos pós-estimulação, após uma sessão única e após quatro sessões repetidas e cumulativas.

Métodos: Este estudo é um ensaio clínico randomizado, duplamente cego e controlado por placebo, envolvendo 21 adultos saudáveis divididos em dois grupos. Um grupo recebeu HD-tDCS anódica (n=11) e o outro recebeu estimulação placebo (n=10). A HD-tDCS foi administrada com uma configuração de elétrodos 4x1, direcionada à região cortical V1, com uma corrente de 2.0 mA durante 20 minutos, em quatro sessões consecutivas. Os participantes foram avaliados em três momentos distintos: antes da estimulação (v0), após uma sessão única (v1) e após as quatro sessões repetidas (v2). As avaliações incluíram medições da BCVA, CS acromática, estrutura retiniana através de tomografia de coerência ótica, função das células ganglionares da retina através do PERG, e integridade funcional do sistema visual através dos VEP.

Resultados: A HD-tDCS anódica sobre o córtex visual primário conduziu a melhorias específicas na CS em função da frequência espacial, em adultos saudáveis. Melhorias após uma sessão única foram evidentes apenas para 3.4 cpd ($g = +0.70$, $p = 0.01$, $q = 0.02$). Ganhos cumulativos significativos foram observados para 2.2, 3.4, 7.1 e 14.2 cpd após quatro sessões, com *effect sizes* moderados a elevados. As comparações entre grupos mostraram tendências favoráveis à estimulação anódica para 2.2 e 3.4 cpd. Os VEP apresentaram *effect sizes* pequenos a moderados, próximos da significância (amplitude cumulativa da onda P100 para 1º: $p = 0.02$, $q = 0.07$, $g = 1.07$). As métricas da BCVA e do PERG apresentaram melhorias cumulativas não significativas no grupo anódico, sem diferenças significativas entre grupos. A estrutura retiniana manteve-se estável ao longo de todas as visitas, sem alterações detetáveis na camada de células ganglionares ou na camada de fibras nervosas da retina.

Conclusões: Estes resultados demonstram que a HD-tDCS anódica aplicada sobre o córtex visual primário pode melhorar a CS em adultos saudáveis, particularmente nas frequências espaciais médias a elevadas, apoiando a sua capacidade de modular a excitabilidade cortical de forma direcionada e cumulativa. Embora as medidas eletrofisiológicas e estruturais se tenham mantido, em grande parte, estáveis, observaram-se tendências para um aumento da responsividade cortical visual. Esta evidência multimodal destaca o potencial de protocolos focais e repetidos de HD-tDCS para induzir alterações funcionais no sistema visual, oferecendo uma base sólida para futuras investigações translacionais em doenças neuro-oftalmológicas clínicas.

Palavras-chave: HD-tDCS anódica, córtex visual primário, adultos saudáveis, sensibilidade ao contraste, abordagem multimodal

Abstract

Introduction: High-definition transcranial direct current stimulation (HD-tDCS) is a non-invasive brain stimulation technique that uses focalized electrical currents to modulate neural activity in targeted brain regions. Through anode and cathode electrode placements to induce unidirectional current flow, a growing body of evidence suggests that electrical stimulation of V1 can enhance visual functions. By targeting V1, which is essential for early-stage visual cortical processing, the aim is to assess visual and cortical outcomes of anodal HD-tDCS in a healthy adult sample. Studying immediate and repeated effects of HD-tDCS on V1 excitability has the purpose to elucidate the mechanisms and potential clinical applications in visual and neurodevelopmental disorders.

Aims: This study aimed to investigate the impact of anodal HD-tDCS over the primary visual cortex on contrast sensitivity (CS) in healthy adults. It also assessed the effects of anodal HD-tDCS on best corrected visual acuity (BCVA), visual evoked potentials (VEP) P100 wave amplitude and implicit time, pattern electroretinography (PERG) P50 and N95 waves amplitude and implicit time, and retinal structure. We evaluated the effects of HD-tDCS by comparing baseline measurements with post-stimulation effects after a single session and after four repeated cumulative stimulation.

Methods: This study is a randomized, double-blind, sham-controlled trial involving 21 healthy adults divided into two groups. One group received anodal HD-tDCS (n=11), and the other sham stimulation (n=10). HD-tDCS was administered using a 4x1 electrode configuration targeting the visual region V1 with a 2.0-mA current for 20 minutes, four consecutive times. Participants were assessed at three different data retrieval timepoints: before the stimulation (baseline), after a single session of stimulation (v1), after the four repeated stimulation sessions (v2). The assessments included measurements of BCVA, achromatic CS, retinal structure through optical coherence tomography, retinal ganglion cell function via PERG, and the functional integrity of the visual system using VEP.

Results: Anodal HD-tDCS over the primary visual cortex led to spatial frequency-specific improvements in CS in healthy adults. Acute improvements were evident only at 3.4 cpd after a single session ($g = +0.70$, $p = 0.01$, $q = 0.02$). Significant cumulative gains were observed at 2.2, 3.4, 7.1, and 14.2 cpd after four sessions, with moderate to large effect sizes. Between-group comparisons showed trends favoring anodal stimulation at

2.2 and 3.4 cpd. VEP showed close to significance small-to-moderate effect sizes (cumulative P100 amplitude at 1º: $p = 0.02$, $q = 0.07$, $g = 1.07$). BCVA and PERG metrics showed non-significant cumulative improvement in the anodal group, with no significant between-group differences. Retinal structure remained stable across all visits, with no detectable changes in the ganglion cell layer or retinal nerve fiber layer.

Conclusions: These findings demonstrate that anodal HD-tDCS over the primary visual cortex can enhance visual CS in healthy adults, particularly at mid-to-high spatial frequencies, supporting its capacity to modulate cortical excitability in a targeted and cumulative manner. While electrophysiological and structural measures remained largely stable, trends toward increased visual cortical responsiveness were observed. This multimodal evidence highlights the potential of focal, repeated HD-tDCS protocols to induce functional changes in the visual system, offering a foundation for future translational research in clinical neuro-ophthalmological diseases.

Keywords: Anodal HD-tDCS, primary visual cortex, healthy adults, contrast sensitivity, multimodal approach

Abbreviations / Acronyms list

Amp. - Amplitude
BCVA - Best Corrected Visual Acuity
BDNF – Brain Derived Neurotrophic Factor
BL - Baseline
cpd - cycles per degree
CS - Contrast Sensitivity
CSF - Contrast Sensitivity Function
dB - decibels
DTL - Dawson-Trick-Litzkow (electrode)
FDR - False Discovery Rate
g - Hedges'g
GABA - Gamma-Aminobutyric Acid
GCL - Ganglion Cell Layer
Glx - Glutamate + Glutamine
HD-tDCS - High-Definition Transcranial Direct Current Stimulation
Hz - Hertz
ISCEV - International Society for Clinical Electrophysiology of Vision
IT. - Implicit Time
LTD - Long-Term Depression
LTP - Long-Term Potentiation
M - Mean
mA/cm² - milliampere per square centimeter
mm - millimeters
ms - milliseconds
mV - millivolts
NIBS - Non-Invasive Brain Stimulation
NMDA - N-Methyl-D-Aspartate (Receptor)
OCT - Optical Coherence Tomography
p - *p*-value
PERG - Pattern Electroretinogram
V1 - Primary Visual Cortex
q - *q*-value
RNFL - Retinal Nerve Fiber Layer
rps - reversals per second
SD - Standard Deviation
tDCS - Transcranial Direct Current Stimulation
tES - Transcranial Electrical Stimulation
v0 - Baseline
v1 - Visit 1
v2 - Visit 2
VEP - Visual Evoked Potential
µm - micrometers
µV – microvolts
Δ - difference or change

Table of Contents

Acknowledgments ..... **v**
Resumo ..... **vi**
Abstract ..... **viii**
Abbreviations / Acronyms list ..... **x**
List of figures ..... **xii**
List of tables ..... **xii**
1. Introduction **13**
2. Objectives **17**
3. Theoretical Background **19**
3.1. Fundamentals of Neuronal Signaling 20
3.2. Neuronal Modulation Through Non-Invasive Brain Stimulation 21
3.2.1. Transcranial Electrical Stimulation Techniques: tDCS and HD-tDCS 23
3.3. Visual Pathway and Visual Network Plasticity 24
4. Materials and Methods **27**
4.1. Study design and Ethical statement 28
4.2. High-definition Transcranial Direct Stimulation Protocol 29
4.3. Data Retrieval 31
4.3.1. Contrast Sensitivity 31
4.3.2 Best Corrected Visual Acuity 32
4.3.3. Visual Evoked Potentials 32
4.3.4. Pattern Electroretinogram 33
4.3.5. Optical Coherence Tomography 34
4.4. Data Analysis 35
5. Results **37**
5.1. Contrast Sensitivity 38
5.2. Visual Evoked Potentials 41
5.3. Pattern Electroretinogram 42
5.4. Best Corrected Visual Acuity 43
5.5. Optical Coherence Tomography 43
5.6. Side-effects Questionnaire and Stimulation Perception 44
6. Discussion **47**
7. Limitations **57**
8. Future Directions **59**
9. Conclusion **61**
10. References **63**

List of figures

Figure 1. Project protocol for HD-tDCS application and data retrieval moments. 29
Figure 2 Electrode positioning protocol. 30
Figure 3. Current flow modeling predictions programed through Soterix Medical software 30
Figure 4. Line plots displaying the changes in contrast sensitivity 39
Figure 5. Mean intensity of the most frequently reported side effects 44

List of tables

Table 1. CS assessed at six spatial frequencies 40
Table 2. P100 amplitude and implicit time at 1º and 0.25º stimulus 41
Table 3. PERG outcomes including P50 and N95 wave amplitude and implicit time and the N95/P50 ratio 42
Table 4. BCVA outcomes in number of letters seen. 43
Table 5. Number of participants reporting HD-tDCS side effects 44
Table 6. Participants' guesses regarding stimulation condition 45

1. Introduction

Introduction

Non-invasive brain stimulation (NIBS) is a growing field in neuroscience research that uses magnetic or safe electrical stimulation techniques to enable the modulation of neural activity in targeted, superficial areas of the human brain. Transcranial electrical stimulation (tES) is one of these non-invasive neuromodulation methods, that involves applying a low-intensity electrical current up until 2 mA to the scalp for a duration of up to 20 minutes. Among different tES approaches, conventional transcranial direct current stimulation (tDCS) uses strategic placement of an anode and a cathode to create a unidirectional stimulation circuit. Typically, the current flows from the anode to the cathode. This potential of modulating neuronal activity resides in the capability to alter neuronal membrane potentials primarily through the opening or closing of voltage-gated ion channels, where anodal (positive current) stimulation tends to bring the resting membrane potential closer to depolarization and cathodal (negative current) stimulation brings it closer to hyperpolarization cathode (Aberra et al., 2023; Bhattacharya et al., 2022; de Venecia & Fresnoza, 2021; Liu et al., 2018). Similarly, high-definition transcranial direct current stimulation (HD-tDCS) employs the same anode and cathode terminology but represents a technique designed to modulate neuronal activity more precisely, and consistently through specific and targeted electrode setups focused on the area of interest. While multiple electrode configurations can be explored, the 4x1 ring montage in HD-tDCS uses four return electrodes surrounding a stimulation electrode that seems to allow a more focused stimulation with reduced likelihood of current dispersion to adjacent cortical regions (Alam et al., 2016; Chen et al., 2023; Kuo et al., 2013; Pereira et al., 2021; Villamar et al., 2013).

Due to such effects, tDCS and HD-tDCS protocols have also been used to assist in the treatment of a range of disorders, showing a neuroprotective and modulator effect in motor, sensory, and cognitive functions in various clinical contexts (Bhattacharya et al., 2022; Mattioli et al., 2024; Sanches et al., 2021). Applying tDCS to cortical visual areas has demonstrated potential in modulating various aspects of visual perception and enhancing visual functions (Bello et al., 2023).

The primary visual cortex (V1), located in the occipital lobe, is the first cortical area to receive and process visual information from the retina and is intrinsically involved in the initial stages of visual perception. Beyond V1, there are two functionally specialized processing pathways: a ventral stream for detail, recognition, and color object vision; and

a dorsal stream for spatial vision and motion perception. Given the hierarchical nature of visual processing, targeting V1 with electrical stimulation could, and already has proven, have an influence in early-stage visual processing and subsequently influence higher-order visual functions (Alam et al., 2016; Bhattacharya et al., 2022; Zito et al., 2015).

In fact, literature illustrated that modulation of visual areas is possible, but its effects are dependent on factors such as stimulation technique, polarity, electrode position, stimulated visual area, subjects age, time of stimulation and pathological or non-pathological contexts. For instance, a review on tES by Bello et al. (2023) reported that anodal stimulation on occipital cortex and V1 area, has significant effects on contrast sensitivity, VEPs P100 wave amplitude, index of cortical excitability and crowding among normally sighted individuals. On the opposite hand, cathodal tDCS, which hyperpolarizes neuronal membranes and reduces cortical excitability, has shown benefits primarily in pathological visual contexts and on motion perception and alertness in V5 of healthy subjects (Antal et al., 2004a, 2006; de Venecia & Fresnoza, 2021; Liu et al., 2018; Wu et al., 2020; Zito et al., 2015).

Despite being a relatively well-studied area, the literature on electrical stimulation over V1 is more prominent in tDCS, giving rise to a question on whether the use of an HD-tDCS montage would increase focality and precision, and reduce current dispersion to adjacent visual areas, improving significantly visual function (Alam et al., 2016). A more targeted approach to V1 could be advantageous to visual function. To our knowledge, HD-tDCS has been applied to the occipital cortex and V1. However, existing research focused on topics such as attentional reorientation and visual crowding, leaving an open window to study its effects in other high and low-level related visual functions (Alam et al., 2016; Arif et al., 2022; Chen et al., 2023).

The positive outcomes of anodal tES in the review from Bello et al. (2023) indicates that its effects on the visual cortex are mostly acute/immediate, however they can persist beyond one stimulation session, with the duration and extent of these effects being influenced by factors such as stimulation duration, number of sessions, and the specific cortical areas targeted. In fact, while most studies report immediate post-stimulation benefits on visual function after one session of stimulation while the ones focused on multiple sessions of tDCS suggest the existence of cumulative effects with repeated stimulation sessions, making it relevant to question if multiple sessions can enhance

already normal visual individuals (Behrens et al., 2017; Bello et al., 2023; Olma et al., 2013).

We hypothesize that comparing the longitudinal data of HD-tDCS V1-induced excitability between pre-stimulation, after a single stimulation and after continuous cumulative stimulation in healthy adults could be beneficial to understand the mechanisms of cortical electrical stimulation and its relationship to stimulation duration. Furthermore, we propose that it is relevant to study the outcomes of anodal HD-tDCS on contrast sensitivity (CS), best corrected visual acuity (BCVA), visual evoked potentials (VEP) P100 amplitude and implicit time, pattern electroretinography (PERG) P50 and N95 amplitudes and implicit times, and retinal structure (neuronal layers) of healthy adults. Most existing tES studies have focused on selected or individual visual metrics, making a multimodal approach a distinctive feature to possible correlations (Bello et al., 2023).

The necessity to understand the fundamental effects of HD-tDCS in V1 of healthy individuals can be beneficial to establish visual normative patterns resulting from electrical stimulation, without the confounding effects of neurological or visual impairments, possibly bringing knowledge for future clinical applications in acquired ophthalmological diseases or neurodevelopmental visual conditions (Antal et al., 2004a; de Venecia & Fresnoza, 2021; Mattioli et al., 2024; Spiegel et al., 2013).

2. Objectives

2. Objectives

Primary aim:

1) To investigate the impact of anodal HD-tDCS over the primary visual cortex (V1) on contrast sensitivity in a healthy sample of adults.

Secondary Aims:

2) To assess the impact of anodal HD-tDCS on best corrected visual acuity (BCVA), VEP P100 wave amplitude and implicit time, PERG P50 and N95 waves amplitude and implicit time, and retinal structure (neuronal layers) in healthy adults.
3) To evaluate the impact of HD-tDCS on visual and cortical outcomes by comparing baseline measurements with effects after a single session, and after four repeated cumulative stimulation sessions.

3. Theoretical Background

3. Theoretical Background

3.1. Fundamentals of Neuronal Signaling

The nervous system relies fundamentally on the transmission of electrical signals for the coordination of perception, cognition, and behavior. These signals are conveyed by neurons, which are electrically excitable cells uniquely adapted for rapid communication over long distances. The ability of a neuron to generate and propagate electrical impulses arises from the intrinsic biophysical properties of its plasma membrane and the activity of specialized ion channels and pumps embedded within it (Bear et al., 2020; Kandel et al., 2021).

In the resting state, a neuron maintains a membrane potential of approximately -65 to -70 millivolts (mV), with the intracellular space negatively charged relative to the extracellular environment. This electrical polarization is primarily established by the sodium-potassium ATPase pump (Na^+/K^+ pump), which actively transports three sodium ions (Na^+) out of the cell and two potassium ions (K^+) into the cell, against their respective concentration gradients. This pump, along with the differential permeability of the membrane to specific ions (especially potassium), creates an electrochemical equilibrium essential for neuronal excitability (Bear et al., 2020; Kandel et al., 2021; Purves et al., 2018).

When a neuron is stimulated by a sufficient external or synaptic input, voltage-gated sodium channels on the membrane rapidly open, allowing Na^+ ions to flow into the cell due to both concentration and electrical gradients. This inward current causes a depolarization of the membrane. If the membrane potential reaches a critical threshold (typically around -55 mV), an action potential is initiated. This is characterized by a rapid and self-sustaining depolarization phase, during which the membrane potential transiently becomes positive, often peaking at values near +30 to +40 mV (Kandel et al., 2021; Purves et al., 2018).

Following the peak of the action potential, voltage-gated potassium channels open, facilitating the efflux of K^+ ions. This outward current repolarizes the membrane, restoring the negative internal voltage. The delayed closure of K^+ channels can cause a brief hyperpolarization phase, where the membrane potential becomes even more negative than the resting level. Subsequently, the Na^+/K^+ pump and passive leak channels

help re-establish the resting membrane potential, rendering the neuron ready to fire again if stimulated (Bear et al., 2016; Purves et al., 2018).

In addition to Na^+ and K^+ dynamics, calcium ions (Ca^{2+}) also play a pivotal role in neuronal signaling. While not typically involved in the initiation of action potentials in most central neurons, voltage-gated calcium channels are activated by depolarization and allow the influx of Ca^{2+}, particularly at presynaptic terminals. The rise in intracellular Ca^{2+} concentration is a key signal that triggers the fusion of synaptic vesicles with the presynaptic membrane, thereby facilitating the release of neurotransmitters into the synaptic cleft. Beyond synaptic transmission, Ca^{2+} also modulates gene expression, enzymatic activity, and intracellular signaling cascades. Ultimately, the propagation of action potentials along the axon and their translation into synaptic activity enables the formation of functional neural circuits. These circuits underline all higher brain functions, from sensory processing to motor output and cognitive integration (Bear et al., 2020; Kandel et al., 2021; Purves et al., 2018).

3.2. Neuronal Modulation Through Non-Invasive Brain Stimulation

Modulation of neuronal excitability is a powerful tool to investigate and potentially modulate neuron fundamental processes in both research and clinical contexts. As mentioned before, at the cellular level, excitability is governed by the resting membrane potential, which reflects the differential permeability of the neuronal membrane to ions and the activity of ion-specific pumps and channels. Small perturbations in ionic homeostasis, particularly changes in extracellular concentrations of potassium or sodium, can significantly affect the membrane potential, thereby altering the likelihood of action potential generation (Bear et al., 2016; Purves et al., 2018). This is the biophysical principle underlying the rationale for various types of Non-Invasive Brain Stimulation (NIBS) modalities where electrical, magnetic or ultrasound stimulus have the ability to modulate brain activity through external physical stimuli without breaching the scalp or skull. As such, transcranial electrical stimulation (tES), transcranial magnetic stimulation (TMS), and transcranial focused ultrasound stimulation (tFUS), allow causally manipulation of cortical excitability and therefore the study of neural mechanisms of cognition, perception, and behavior (Antal et al., 2022; Bhattacharya et al., 2022; Mattioli et al., 2024; Sanches et al., 2021).

At the synaptic level, communication between neurons occurs via neurotransmitter release at specialized junctions. Upon the arrival of an action potential at the presynaptic terminal, synaptic vesicles fuse with the membrane, releasing neurotransmitters into the synaptic cleft. These molecules bind to postsynaptic receptors, eliciting changes in the postsynaptic membrane potential and influencing subsequent neuronal activity. Synaptic strength, a critical determinant of signal efficacy, is modifiable through experience-dependent plasticity. This plasticity occurs primarily in two forms: Hebbian and homeostatic. (Bear et al., 2020; Kandel et al., 2021; Purves et al., 2018).

Hebbian plasticity, classically summarized by the principle "cells that fire together wire together," entails the activity-dependent strengthening (LTP) or weakening (LTD) of synaptic connections, forming a positive feedback loop that enhances the representation of salient stimuli. However, unchecked Hebbian mechanisms risk destabilizing overall network function by amplifying activity beyond optimal limits. In contrast, homeostatic plasticity provides a counter-regulatory process that maintains neuronal stability. This form of plasticity globally scales synaptic strengths across the neuronal membrane, preserving relative differences between synapses established by Hebbian changes, while preventing excitotoxicity or network silencing. Together, these two complementary forms of plasticity enable the nervous system to remain both adaptive and stable (Bear et al., 2020; Kandel et al., 2021).

Critically, the effects of NIBS are not confined to the targeted cortical region. Due to the highly interconnected nature of neural networks, local modulation can lead to functionally meaningful changes in distal brain regions through polysynaptic pathways. This network-level impact underscores the relevance of NIBS for investigating not only local cortical dynamics but also global neural communication patterns. Such properties are particularly relevant to sensory systems such as vision, where processing depends on the coordinated activity of anatomically and functionally distinct areas (Perin et al., 2020)

While NIBS includes several techniques, each with different physical principles and neural effects, the present work focuses specifically on the neuromodulatory effects and properties of transcranial electrical stimulation (tES).

3.2.1. Transcranial Electrical Stimulation Techniques: tDCS and HD-tDCS

Among the various modalities of NIBS, tES encompasses a range of techniques that apply low-intensity electrical currents to modulate neuronal excitability across cortical networks. These currents are delivered through electrodes positioned on the scalp that are capable of inducing changes in both local and distributed brain activity without directly generating action potentials. Instead, tES can alter neuronal membrane potentials, thereby influencing the likelihood of neural firing in an activity-dependent manner (Dayan et al., 2013; Karabanov et al., 2015; Mattioli et al., 2024).

tES itself includes several distinct subtypes, each defined by the waveform of the applied current. The most widely studied and implemented forms include transcranial direct current stimulation (tDCS), transcranial alternating current stimulation (tACS), and transcranial random noise stimulation (tRNS). These approaches differ in their physiological mechanisms and application parameters, though they share the common goal of non-invasively modulating cortical excitability to explore brain-behavior relationships or promote neuroplastic changes in both healthy individuals and clinical populations (Bhattacharya et al., 2022; Mattioli et al., 2024).

In conventional tDCS, a direct current, typically ranging from 0.5 to 2 mA, is applied through at least one anodal (positive) and one cathodal (negative) electrode. The current flows unidirectionally, resulting in polarity-specific changes in neuronal excitability: anodal stimulation typically induces depolarization and facilitates excitability, whereas cathodal stimulation induces hyperpolarization and tends to suppress neural activity (Mattioli et al., 2024; Stagg et al., 2009; Stagg & Nitsche, 2011). However, due to the relatively large size of sponge electrodes used in traditional tDCS (commonly 25-35 cm^2), the resulting current distribution tends to be diffuse, potentially affecting broader cortical regions than intended (Kuo et al., 2013; Villamar et al., 2013).

To improve spatial precision and current focality, high-definition transcranial direct current stimulation (HD-tDCS) was developed. HD-tDCS employs smaller, gel-based electrodes arranged in specific configurations to concentrate the electric field over a targeted cortical area. The most frequently used configuration is the 4 x 1 ring montage, in which the central electrode (defining the stimulation polarity) is surrounded by four equidistant return electrodes. This layout allows for a more confined and consistent current flow, thereby reducing stimulation of adjacent brain regions and enhancing the

anatomical specificity of the intervention (Alam et al., 2016; Hampstead et al., 2020; Kuo et al., 2013; Müller et al., 2023; Villamar et al., 2013)

Modulation by tDCS or HD-tDCS can be categorized based on the polarity of the applied current into two primary forms: anodal and cathodal stimulation. These polarities elicit distinct physiological effects by modulating neuronal excitability in a directionally specific manner. These excitability shifts are not only electrophysiological but also neurochemical in nature. Anodal stimulation has been found to decrease levels of the inhibitory neurotransmitter γ-aminobutyric acid (GABA), while simultaneously increasing concentrations of glutamate and glutamine (Glx), which are key mediators of excitatory synaptic transmission (Karabanov et al., 2015; Liu et al., 2018; Stagg et al., 2009; Stagg & Nitsche, 2011). Conversely, cathodal tDCS has been associated with a downregulation of glutamatergic activity, contributing to its overall inhibitory effects. These alterations in neurotransmitter balance are thought to mediate the long-lasting aftereffects of stimulation by shifting the excitatory-inhibitory equilibrium within cortical networks.effects (Alam et al., 2016; Stagg et al., 2009).

Importantly, the enduring neuroplastic outcomes induced by tDCS are believed to reflect mechanisms analogous to long-term potentiation (LTP) and long-term depression (LTD). Specifically, anodal tDCS may promote LTP-like synaptic strengthening, while cathodal tDCS may facilitate LTD-like synaptic weakening. These plastic processes are crucial for experience-dependent cortical reorganization and are likely to be the basis the behavioral and functional enhancements observed following stimulation (Frase et al., 2021; Karabanov et al., 2015; Yamada & Sumiyoshi, 2021).

3.3. Visual Pathway and Visual Network Plasticity

Vision plays a fundamental role in perception and interaction with the surrounding environment, constituting one of the most elaborate sensory systems in humans. While the human eye serves as the initial gateway for visual stimuli, the process of vision itself is governed by a highly specialized and hierarchically structured neural system that integrates multiple cortical and subcortical areas. The retina, located at the posterior segment of the eye, is the first neural substrate in this pathway. It is composed of photoreceptors (rods and cones), interneurons, and retinal ganglion cells (RGCs), which together convert incident light into neural signals through a process known as

phototransduction. Once converted, these signals are relayed by RGC axons, forming the optic nerve that carries the information toward the lateral geniculate nucleus (LGN) of the thalamus (Bear et al., 2020; Kandel et al., 2021; Purves et al., 2018).

From the LGN, thalamocortical projections transmit visual information to the primary visual cortex (V1), situated in the calcarine sulcus of the occipital lobe and corresponding to Brodmann area 17. This region represents the first cortical processing site where binocular information is synthesized and further decomposed into distinct features such as orientation, spatial frequency, and edge detection. The cortical surface of V1 is organized in a retinotopic fashion, preserving the spatial topology of the visual scene. Notably, the foveal region, responsible for high acuity vision, occupies a disproportionately large cortical area compared to peripheral retinal inputs, a phenomenon known as cortical magnification (Bear et al., 2020; Kandel et al., 2021; Purves et al., 2018).

Beyond V1, visual information is distributed to a constellation of extrastriate areas forming the visual association cortices. These regions are specialized for progressively complex computations and are broadly categorized into two major processing streams. The ventral stream, projecting to the inferotemporal cortex via areas V2 and V4, facilitates object recognition and feature abstraction, and is often referred to as the "what" pathway. Conversely, the dorsal stream extends toward the posterior parietal cortex, primarily through V3 and V5/MT, and mediates spatial localization, motion processing, and visuomotor coordination, thus earning the designation of the "how" pathway (Gallivan & Goodale, 2018). Although functionally distinct, these pathways are interdependent and interact dynamically, ensuring the coherent interpretation of visual stimuli under varying environmental and behavioral demands (Bear et al., 2020; Kandel et al., 2021; Purves et al., 2018).

Literature has also demonstrated that visual processing is not solely feedforward but involves bidirectional communication between the retina and the cortex. While retinal ganglion cells transmit visual input to the lateral geniculate nucleus and onward to the visual cortex, feedback loops from the cortex, particularly V1, to subcortical structures (like the LGN) and even to the retina via sparse retinopetal projections also exist (Briggs & Usrey, 2008; Repérant et al., 2006; Köves & Csáki, 2024). These descending pathways, although limited in number in primates, are often neuromodulatory (ex. histaminergic and serotonergic) and influence retinal function by adjusting sensitivity, contrast, and

adaptation in accordance with external stimulus, circadian rhythms, or behavioral demands (Warwick et al., 2024; Köves & Csáki, 2024). Functional evidence shows that cortical activity can modulate retinal output indirectly via thalamic relay modulation (Murata & Colonnese, 2016) or directly through neuromodulatory systems (Tang et al., 2016), contributing to retinal adaptation and perceptual efficiency. This reciprocal exchange is essential for dynamic visual processing, suggesting that the visual system operates as an integrated, adaptive circuit rather than a strictly hierarchical one.

The visual cortex can also show adaptability and neuroplasticity. In early postnatal development, the visual cortex undergoes a critical period of heightened plasticity when sensory experience induces structural and functional synaptic reorganization, profoundly shaping neural circuits. During this phase, synaptic plasticity is heightened, driven by NMDA receptor activity, experience-dependent synaptic pruning, and a dynamically shifting balance between excitatory and inhibitory neurotransmission. A key regulator of this window is GABAergic inhibition where its maturation triggers the onset of the critical period, while excessive inhibitory tone contributes to its closure (Antal et al., 2011; Duménieu et al., 2021; Hooks & Chen, 2007; Rosa et al., 2013; Sale et al., 2010).

As the visual cortical circuits become less malleable and plasticity periods gradually close in adulthood, the mechanisms of action of tES have shown promise in reopening windows of neuroplasticity in the mature visual cortex. These techniques have the ability to modulate cortical excitability through subthreshold polarization of neurons and their effects appear to depend on mechanisms similar to Hebbian plasticity, including NMDA receptor activation and shifts in GABA concentration (Castaldi et al., 2020; Ding et al., 2016; Spiegel, Li, et al., 2013). Specifically, anodal tDCS can reduce GABA levels and increase excitability in visual areas, possibly creating neurochemical conditions that resemble those found during the critical period. tES capacity to facilitate functional improvements by reactivating latent plastic potential may represent a viable strategy for extending visual plasticity beyond developmental constraints and facilitating functional reorganization in the adult brain. Collectively, tES approaches represent a viable tool for inducing visual plasticity in adulthood, potentially offering rehabilitative value even after the closure of the traditional critical period, therefore holding substantial promise not only for visual enhancement in healthy individuals but also for therapeutic applications in visual disorders (Antal et al., 2011; Castaldi et al., 2020; Frase et al., 2021).

4. Materials and Methods

4. Materials and Methods

4.1. Study design and Ethical statement

The study followed a randomized, double-blind, sham-controlled design. After an eligibility visit, twenty one healthy adults (15 females) with a mean age of 20.29 ± 1.65 years [18-25 years] were randomly divided into two groups with an allocation ratio of 1:1 (11 in the Anodal HD-tDCS group and 10 in the Sham HD-tDCS group). Stratified randomization was used to minimize possible differences between gender and age across groups; thus, the two groups did not differ in age (p>0.05) (Anodal 20.45 ± 1.21 years; Sham 20.10 ± 2.08 years) and had the same gender distribution (3 males per group).

Inclusion criteria included ages between 18 and 40 years old, and BCVA greater than 0.8. Exclusion criteria included the presence of ophthalmological or neuro-ophthalmological pathologies, eye surgery within the six months prior to the baseline assessment, diabetes mellitus even without diabetic retinopathy, inability to cooperate during tests, high ametropias (sphere ≥ ±4D; cylinder ≥ ±2D), head trauma history, seizures, or frequent headaches, having electrical or electronic implants (e.g. cardiac pacemaker), psychiatric disorders including current depression, metallic artifacts in the head (except dental implants), chronic pharmacological therapy, previous treatment with tDCS or other NIBS techniques, pregnancy or planning to become pregnant during the study period, and abuse of alcohol, drugs, or other illicit substances in the six months preceding the study.

Both groups underwent HD-tDCS with daily sessions lasting 20 minutes, four times within one week (s1, s2, s3 and s4). Group 1 received anodal (active) HD-tDCS applied to the primary visual cortex region, while Group 2 received sham HD-tDCS (placebo) to the same region. Data retrieval was made at baseline/pre-stimulation (v0), after one single stimulation session (v1) and after four cumulative stimulation sessions (v2) (Figure 1). Stimulation sessions occurred 24 hours apart from each other to ensure consistency. In all moments of data acquisition, the outcomes of HD-tDCS on achromatic contrast sensitivity, BCVA, neuronal retinal layers thicknesses, retinal ganglion cell function and functional integrity of the visual system were evaluated.

This study was approved by the Ethics Review Board of the Polytechnic University of Porto - School of Health (E2S-IPP) under the approval number CE0084E. All procedures were conducted in accordance with the principles outlined in the Declaration of Helsinki. Prior to participation, all individuals received a detailed explanation of the study

procedures and provided written informed consent. Participant data were collected, processed, and stored in compliance with the principles of the General Data Protection Regulation (Regulamento Geral de Proteção de Dados - RGPD).

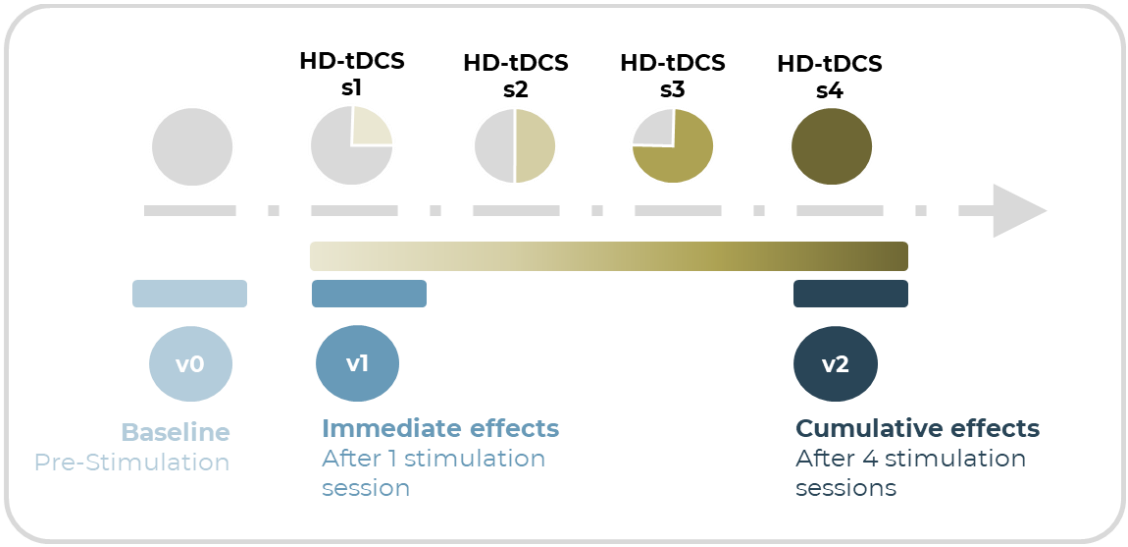

Figure 1. Project protocol for HD-tDCS application and data retrieval moments.

4.2. High-definition Transcranial Direct Stimulation Protocol

HD-tDCS was delivered using a 4x1 ring configuration targeting the visual cortex region (Oz), according to the international 10/20 system. Stimulation was administered using the Soterix MxN-33 HD-tES stimulator (Model 3200C, Soterix Medical Inc., New York, United States), programmed through the manufacturer's Stimulation Controller application (HD-SC app). The central electrode was positioned over Oz (anode) and surrounded by four electrodes of opposite polarity (cathodes) near the parieto-occipital junction (PO3, PO4, PO7, and PO8) (Figure 2). Additionally, a reference electrode was placed at CPz to serve as a stable return node for current monitoring and to promote symmetrical current distribution without interfering with the target stimulation region. This montage closely followed the protocol described by Arif et al. (2022) which was designed to maximize current delivery to early visual areas within the occipital cortex, while minimizing stimulation of adjacent parietal and temporal areas.

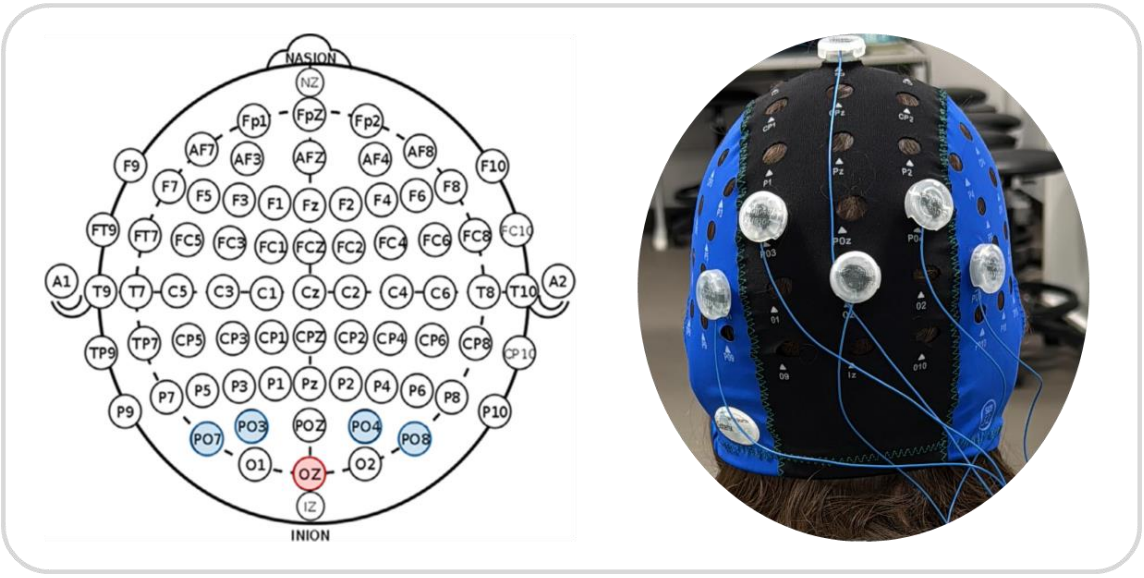

Figure 2 Electrode positioning protocol following Arif et al., 2022 protocol (positive electrode over Oz, negative electrodes over PO3, PO4, PO7, and PO8 and reference over CPz).

The resulting electric field and current flow generated by this montage were also confirmed using the HD-Targets software (Soterix Medical, Inc., New York, United States), as seen in Figure 3. All electrodes used were Soterix Medical HD-GEL Ag/AgCl electrodes with an external diameter of 1.2 cm, corresponding to an estimated contact area of 1.13 cm^2. A total current of 2.0 mA was applied, resulting in a current density of approximately 1.77 mA/cm^2 at the anodal electrode and 0.44 mA/cm^2 at each of the four cathodes. Electric field modeling indicated a mean intracranial field strength of approximately 0.3 V/m within the occipital cortex.

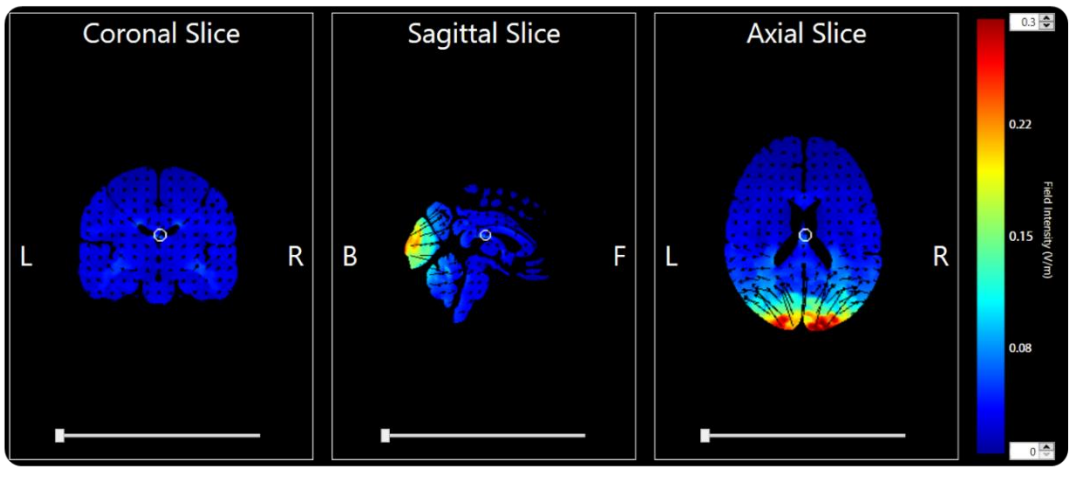

Figure 3. Current flow modeling predictions programed through Soterix Medical software

Participants assigned to the anodal stimulation group received 20 minutes of HD-tDCS at an intensity of 2.0 mA. Stimulation included a 30-second ramp-up and a 30-second ramp-down phases, with continuous direct current applied between these periods. In the sham (placebo) group, the same electrode montage and stimulation parameters were used; however, current was only delivered during the initial 30-second ramp-up and final 30-second ramp-down phases, with no active stimulation in the intervening period. This approach mimics the sensory experiences of active stimulation without inducing potential neuromodulatory effects. Both participant and the researcher operating the stimulator were blinded to the stimulation condition in each session to ensure a double-blind experimental design.

Before and after each stimulation session, safety, and tolerability assessments of HD-tDCS stimulation were conducted using an adapted safety questionnaire (Brunoni et al., 2011; Reckow et al., 2018). This questionnaire consisted of ten commonly reported side effects (headache, neck pain, scalp pain, tingling, itching, burning sensation, skin redness, sleepiness, trouble concentrating, and acute mood changes) as well as an "other" category that allows participants to describe other experiences/sensations. The questionnaire requested participants to rate the intensity of side effects (0 = absent to 3 = severe) when present and whether they think it was HD-tDCS related or not. Additionally, after completing the questionnaire, participants stated which stimulation condition they believe they have received.

4.3. Data Retrieval

Data collection occurred at baseline (v0) and immediately following stimulation during v1 and v2. To minimize temporal bias and ensure consistency across participants, all measurements were performed in a fixed sequential order: CS, VEP, PERG, OCT, and BCVA. The data acquisition process was completed within 120 minutes of stimulation for all participants. This post-stimulation time window falls well within the period considered optimal for capturing offline neurophysiological effects of HD-tDCS (Kuo et al., 2013).

4.3.1. Contrast Sensitivity

Contrast sensitivity was evaluated using the MonCV3 device (MetroVision, Perenchies, France), which employs vertical sine-wave gratings with computer-controlled parameters

including luminance, contrast, and spatial frequency. Each grating was presented progressively, with contrast increasing in steps of 0.25 dB to avoid detection biases due to abrupt contrast changes. Participants were instructed to press a response button upon detecting the presence of the grating pattern.

Static (0 Hz temporal frequency) tests were performed monocularly at each data acquisition point under standardized photopic conditions (mean luminance of 80 cd/m²), with participants wearing their best optical correction for the testing distance (2 meters). The baseline tests were performed two times before the final acquisition in order to eliminate learning bias. Additionally, for each trial, the device averaged three measured values for each of the 6 different spatial frequencies tested (high to low spatial frequencies: 14.2 - 7.1 - 3.4 - 2.2 - 1.1 - 0.6 in cycles per degree (cpd)). The resulting contrast sensitivity function (CSF) indicated all participant responses at each spatial frequency against the corresponding contrast threshold (expressed in dB).

4.3.2 Best Corrected Visual Acuity

Visual acuity was measured under standardized photopic conditions using an ETDRS-style chart displayed on a calibrated 17-inch LED-backlit screen (MediWorks Vision Chart C901, Shanghai, China) positioned at a distance of 6 meters. The chart adhered to standardized ETDRS specifications, consisting of 12 rows of five Sloan letters each, with a geometric progression of letter size between rows. Participants used their best optical correction for all measurements. Monocular visual acuity was tested by presenting the chart to one eye while occluding the fellow eye. To minimize memorization effects, different chart versions were employed across visits and between eyes. Participants were instructed to identify each optotype sequentially, and responses were recorded by the examiner using a scoring sheet. BCVA was determined based on the total number of correctly identified letters, with a maximum score of 60 letters at baseline, v1 and v2.

4.3.3. Visual Evoked Potentials

To assess the functional integrity of the visual pathway from the retina to the primary visual cortex, pattern-reversal VEP´s were recorded using the Tomey EP-1000 Pro system

(Tomey GmbH, Japan), following the guidelines established by the International Society for Clinical Electrophysiology of Vision (ISCEV) 2016 standards (Odom et al., 2016).

High-contrast black-and-white checkerboard stimuli with check sizes of 1° (large) and 0.25° (small) were presented on a monitor positioned 80 cm from the participants, ensuring that the visual field covered at least 15°. Pattern reversals occurred at a rate of 2 reversals per second (2 rps), equivalent to 1 Hz. The mean luminance of the stimuli was maintained at 50 cd/m², with a Michelson contrast between white and black squares exceeding 80%.

Electrodes were positioned according to the International 10/20 system, relative to the nasion and inion, and proportionally adjusted to head size. The active electrode was placed over the visual cortex at Oz (midline occipital), the reference electrode at Fz (midline frontal), and the ground electrode at Cz (vertex). Electrode impedances were ideally kept below 5 kΩ. VEP signals were amplified, band-pass filtered between 1 and 100 Hz, and averaged over 100 stimulus presentations to enhance the signal-to-noise ratio. Participants were seated comfortably in a dimly lit room and instructed to maintain fixation on a central target throughout the recording. Each eye was tested separately while the fellow eye was occluded. Two recordings were made per eye with participants wearing their best optical correction for the testing distance: one recording using the 0.25° checks and one using the 1° checks.

Recordings were obtained at baseline, and within one hour following HD-tDCS stimulation at v1 and v2. The implicit times and amplitudes of the P100 wave for each check size were extracted for analysis.

4.3.4. Pattern Electroretinogram

PERG recordings were performed using the Tomey EP-1000 Pro system (Tomey GmbH, Japan) and in accordance with the most recent ISCEV protocol (2024) in order to study macular and ganglion cell function (Thompson et al., 2024). Active electrodes (DTL fiber electrodes) were placed in the lower conjunctival fornix of each eye, positioned beneath the lower eyelid without touching the cornea. Electrodes were carefully secured to minimize movement artifacts. Reference electrodes (negative) were positioned on the skin near the ipsilateral outer canthus (temporal side) of the eye being tested, to reduce

interference from cortical potentials. The ground electrode was placed on a neutral site (forehead). Electrode impedance was maintained below 5 kΩ for all recordings.

The visual stimulus consisted of high-contrast (≥80%) black-and-white checkerboard patterns presented at a mean luminance of 50 cd/m² on a monitor located 80 cm from the participant. The check size was 0.75°, subtending a visual angle of 15° × 15°. Pattern reversals occurred at a rate of 4 reversals per second (2 Hz).

Participants were seated comfortably in a dimly lit room and instructed to fixate on a central target throughout the test. Three binocular recordings were obtained without pharmacological pupil dilation, with participants wearing their best optical correction for the testing distance. The electrophysiological signals were also amplified, band-pass filtered between 1 and 100 Hz, and sampled at a rate of 1 kHz.

Consistent with the remaining procedures, PERG recordings were performed at baseline, v1 and v2, each within one hour following HD-tDCS. The amplitudes and implicit times of the P50 and N95 components were extracted, reflecting the functional integrity of the macula and retinal ganglion cells, respectively.

4.3.5. Optical Coherence Tomography

Structural macular and optic nerve scans from each eye were acquired through high-resolution Spectral Domain Optical Coherence Tomography (OCT) using the Optopol Copernicus Revo 60 SD-OCT device (Optopol Technology Sp. z o.o., Zawiercie, Polska, software version 11.5.1) which operates at an 840 nm superluminescent diode source, with a transverse resolution of 12 µm, axial resolution of 5 µm, and a scanning speed of 80,000 A-scans per second. OCT scans were obtained at Baseline, V1 and V2 within 2 hours following HD-tDCS application.

A 7 × 7 mm macular cube 3D scan was acquired to assess total macular thickness and ganglion cell layer (GCL) thickness. Macular thickness measurements were extracted from the ETDRS grid division into superior, inferior, nasal and temporal sectors to deliver average thickness measures from the central 1mm, 3mm and 6mm. GCL thickness was extracted from the central six perifoveal sectors given by the device.

The 6x6mm 3D optic disc protocol was performed to assess Retinal Nerve Fiber Layer (RNFL) thickness measurements using a circular peripapillary map corresponding to the

overall average thickness and the following optic nerve head sectors: temporal, superior, nasal, and inferior. Optic disc parameters were also extracted including cup/disc ratio and their associated volumes and depths.

All scans were processed using the built-in segmentation algorithms of the Optopol Copernicus Revo 60 software. Manual corrections were applied when necessary to ensure accurate delineation of retinal layers and optic disc margins. Each eye was scanned twice per session and only scans with a minimum image quality index (QI) ≥9/10 and free from artifacts or segmentation errors were included for analysis.

4.4. Data Analysis

Statistical analyses were performed were performed using IBM SPSS Statistics version 29 (IBM Corp., Armonk, NY, USA). For all metrics the mean value from both eyes was used for each subject for all the analysis at each timepoint (v0, v1 and v2). Data was reported as mean ± standard deviation (SD), unless otherwise specified. The normality of each variable and change score was assessed using the Shapiro-Wilk test.

To evaluate the acute effect of stimulation, paired-sample t-tests (or Wilcoxon signed-rank tests for non-normal data) were used to compare baseline (v0) with post-first stimulation (v1) values within each group (anodal, sham). The cumulative effect was assessed by comparing baseline with post-fourth stimulation (v2) values within each group using the same approach.

To determine whether anodal stimulation led to greater improvement than sham, individual change scores were calculated as the difference between post-stimulation and baseline values (v1-v0 for acute, v2-v0 for cumulative effects). These change scores were compared between groups using independent samples t-tests (or Mann-Whitney U tests if assumptions were not met).

Multiple comparisons correction was applied using the Benjamini-Hochberg False Discovery Rate (FDR) procedure, within each metric, with significance set at $q < 0.05$. Hedges' g was calculated for all effect sizes.

5. Results

5. Results

5.1. Contrast Sensitivity

Contrast sensitivity was evaluated at six spatial frequencies (0.55, 1.1, 2.2, 3.4, 7.1, and 14.2 cycles per degree) for both anodal and sham groups (for more details see Figure 4 and Table 1)

Effects after a single session: There were no effects after only a single stimulation session in either frequency, except for the 3.4 cpd spatial frequency (Δv1-v0 = +0.95 ± 1.42, p = 0.007, q = 0.020, g = +0.70) in the anodal group.

Effects after four repeated cumulative sessions: In the anodal group, a significant cumulative improvement in CS was detected at 2.2 cpd (Δv2-v0 = +2.09 ± 1.56, p = 0.001, q = 0.007, g = +1.25), 3.4 cpd (Δv2-v0 = +1.50 ± 1.06, p = 0.001, q = 0.006, g = +1.28), 7.1 cpd (Δv2-v0 = +1.82 ± 1.95, p = 0.001, q = 0.006, g = +1.17) and also 14.2 cpd (Δv2-v0 = +1.45 ± 1.36, p = 0.005, q = 0.033, g = +0.97). No significant within-group changes were observed at the lowest frequencies (0.55 and 1.1 cpd) after FDR correction (q-value), although 1.1 cpd showed a borderline value (q = 0.059).

In the sham group, close to significance cumulative improvements were also observed at several frequencies, but the magnitude of improvement was smaller than in the anodal group and did not reach significance at either frequency.

Between group comparisons: There was a trend in acute effect in favor of anodal stimulation at 3.4 cpd (Δv1-v0: g = +0.81, p = 0.055, q = 0.078), and a trend toward significance for the cumulative effect at both 2.2 cpd (g = +0.80, p = 0.069, q = 0.083) and 3.4 cpd (g = +0.82, p = 0.065, q = 0.078). No significant between-group differences were detected at other frequencies after FDR correction.

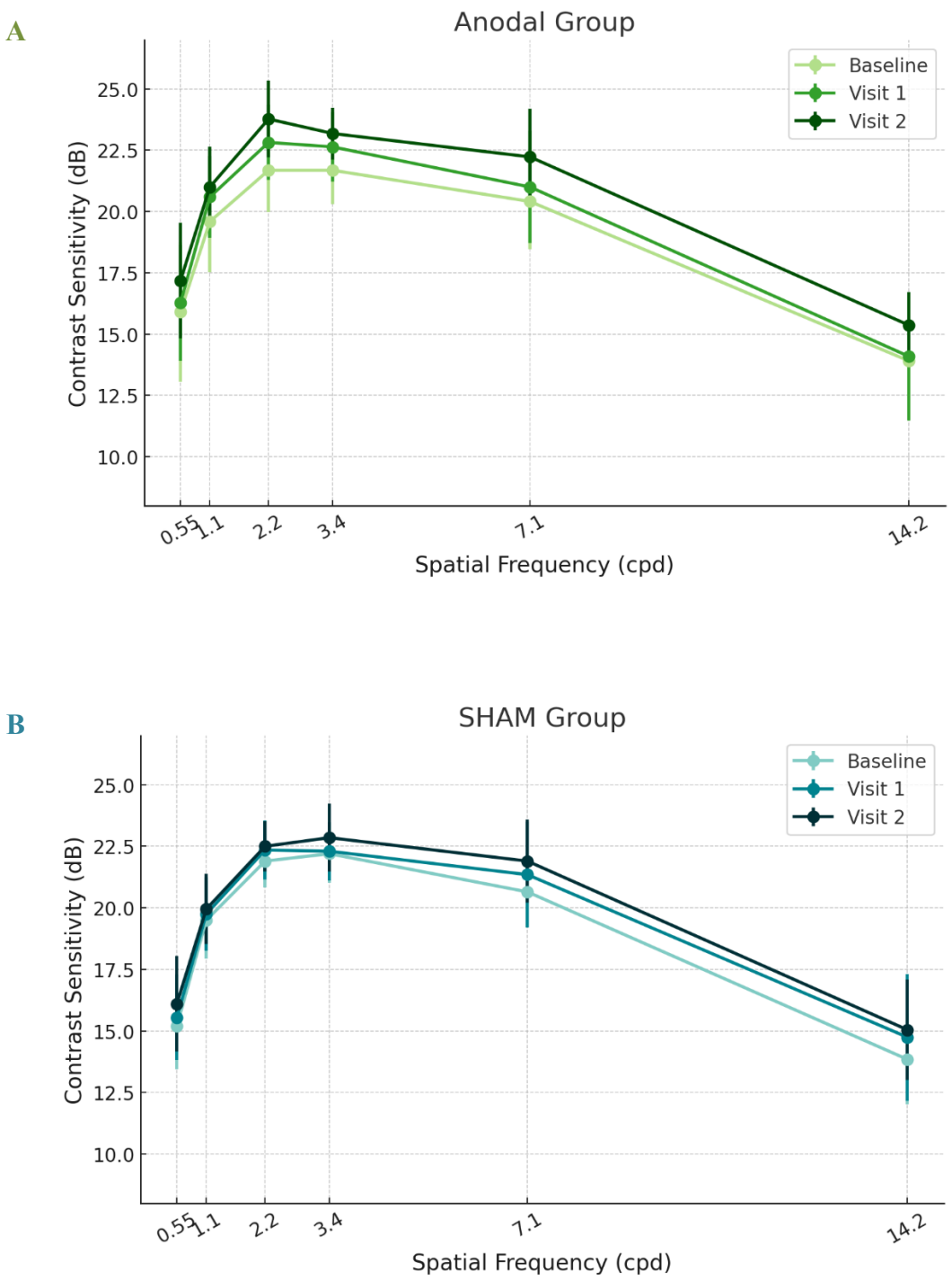

Figure 4. (A and B) Line plots displaying the changes in contrast sensitivity at six spatial frequencies (0.55, 1.1, 2.2, 3.4, 7.1, and 14.2 cpd) following anodal and sham HD-tDCS. Mean ± SD CS values at baseline, after one stimulation session (visit 1), and after four sessions (visit 2).

			Baseline	Visit 1			Visit 2		
	Group	n	v0 [mean ± SD]	v1 [mean ± SD]	Δ(v1-v0) (*p*, *q*, *g*)	Between group Δv1-v0	v2 [mean ± SD]	Δ(v2-v0) (*p*, *q*, *g*)	Between group Δv2-v0
0.55 cpd (dB)	**Anodal**	11	15.91 ± 2.84	16.27 ± 2.35	+0.36 (0.72, 0.72, +0.21)	*p* = 0.67 *q* = 0.72 *g* = 0.01	17.18 ± 2.36	+1.27 (0.03, 0.15, +0.72)	*p* = 0.56 *q* = 0.72 *g* = 0.24
	Sham	10	15.20 ± 1.75	15.55 ± 1.74	+0.35 (0.35, 0.71, +0.28)		16.10 ± 1.94	+0.90 (0.05, 0.15, +0.64)	
1.1 cpd (dB)	**Anodal**	11	19.59 ± 2.06	20.59 ± 1.67	+1.00 (0.07, 0.13, +0.57)	*p* = 0.56 *q* = 0.56 *g* = 0.36	21.00 ± 1.64	+1.41 (0.02, 0.06, +0.79)	*p* = 0.25 *q* = 0.30 *g* = 0.49
	Sham	10	19.25 ± 1.48	19.75 ± 1.50	+0.50 (0.13, 0.19, +0.48)		20.00 ± 1.41	+0.75 (0.01, 0.11, +0.94)	
2.2 cpd (dB)	**Anodal**	11	21.68 ± 1.69	22.82 ± 1.52	+1.14 (0.02, 0.06, +0.62)	*p* = 0.78 *q* = 0.78 *g* = 0.31	23.77 ± 1.56	**+2.09 (0.00, 0.01, +1.25)**	*p* = 0.07 *q* = 0.08 *g* = 0.80
	Sham	10	21.75 ± 1.16	22.45 ± 1.26	+0.70 (0.03, 0.07, +0.71)		22.75 ± 1.18	+1.00 (0.01, 0.08, +0.88)	
3.4 cpd (dB)	**Anodal**	11	21.68 ± 1.38	22.64 ± 1.42	**+0.95 (0.01, 0.02, +0.70)**	*p* = 0.06 *q* = 0.08 *g* = 0.81	23.18 ± 1.06	**+1.50 (0.00, 0.01, +1.28)**	*p* = 0.07 *q* = 0.08 *g* = 0.82
	Sham	10	22.20 ± 1.18	22.30 ± 1.18	+0.10 (0.64, 0.64, +0.14)		22.85 ± 1.38	+0.65 (0.05, 0.08, +0.64)	
7.1 cpd (dB)	**Anodal**	11	20.41 ± 1.93	21.00 ± 2.29	+0.59 (0.28, 0.36, +0.32)	*p* = 0.87 *q* = 0.87 *g* = -0.07	22.23 ± 1.95	**+1.82 (0.00, 0.01, +1.17)**	*p* = 0.30 *q* = 0.36 *g* = 0.38
	Sham	10	20.65 ± 1.43	21.35 ± 2.15	+0.70 (0.14, 0.28, +0.47)		21.90 ± 1.70	+1.25 (0.02, 0.07, +0.77)	
14.2 cpd (dB)	**Anodal**	11	13.91 ± 2.42	14.09 ± 2.63	+0.18 (0.43, 0.52, +0.20)	*p* = 0.13 *q* = 0.20 *g* = -0.68	15.36 ± 1.36	**+1.45 (0.01, 0.03, +0.97)**	*p* = 0.70 *q* = 0.70 *g* = 0.16
	Sham	10	13.85 ± 1.83	14.75 ± 2.57	+0.90 (0.04, 0.09, +0.68)		15.05 ± 2.03	+1.20 (0.04, 0.09, +0.67)	

Table 1. CS assessed at six spatial frequencies (0.55, 1.1, 2.2, 3.4, 7.1, and 14.2 cpd - Table entries report mean ± SD values for CS parameters across visits: baseline (v0), after a single HD-tDCS session (v1), and after four sessions (v2). Changes from baseline (Δ) and associated statistics (p, FDR q-value within each CS metric, and Hedges' g) assess acute (Δv1-v0) and cumulative (Δv2-v0) CS responses to each associated stimulation condition. Between-group statistics compare the change in CS responses from Anodal compared to Sham. Notes: Bold fonts highlight any significant effects of HD-tDCS. Significance was set at $q < 0.05$.

5.2. Visual Evoked Potentials

VEPs were analyzed for P100 amplitude and implicit time at 1º and 0.25º stimulus sizes at baseline, visit 1, and visit 2, for both the anodal and sham groups (Table 2). No statistically significant single or cumulative within-group changes were observed in any VEP metric after FDR correction (all q > 0.05). The largest effect was a cumulative increase in P100 amplitude at 1º in the anodal group (Δ = +1.34, p = 0.01, q = 0.06, g = 0.19), and a cumulative increase in P100 amplitude at 1º check sizes for the between-group comparison (Δ = +1.91, p = 0.02, q = 0.07, g = 1.07), but these did not reach statistical significance after correction.

			Baseline	Visit 1			Visit 2		
	Group	n	v0 [mean ± SD]	v1 [mean ± SD]	Δ(v1-v0) (*p*, *q*, *g*)	Between group Δv1-v0	v2 [mean ± SD]	Δ(v2-v0) (*p*, *q*, *g*)	Between group Δv2-v0
P100 Amp. 1º (μV)	**Anodal**	11	16.24 ± 6.83	17.42 ± 8.48	+1.18 (0.21, 0.42, 0.15)	*p* = 0.37 *q* = 0.50 *g* = 0.39	17.58 ± 6.63	+1.34 (0.01, 0.06, 0.19)	*p* = 0.02 *q* = 0.07 *g* = 1.07
	Sham	10	20.16 ± 4.61	20.14 ± 3.26	-0.02 (0.99, 0.99, -0.00)		19.58 ± 5.21	-0.58 (0.42, 0.50, -0.11)	
P100 IT. 1º (ms)	**Anodal**	11	105.03 ± 4.34	105.57 ± 3.16	+0.54 (0.60, 0.72, 0.14)	*p* = 0.39 *q* = 0.72 *g* = 0.38	105.29 ± 3.99	+0.25 (0.74, 0.74, 0.06)	*p* = 0.20 *q* = 0.74 *g* = 0.55
	Sham	10	107.63 ± 2.82	106.95 ± 2.36	-0.68 (0.50, 0.60, 0.25)		103.27 ± 5.34	-0.12 (0.93, 0.97, -0.03)	
P100 Amp. 0.25º (μV)	**Anodal**	11	18.93 ± 7.79	20.57 ± 9.79	+1.64 (0.20, 0.93, 0.18)	*p* = 0.36 *q* = 0.93 *g* = 0.40	18.99 ± 8.45	+0.06 (0.93, 0.93, 0.01)	*p* = 0.64 *q* = 0.27 *g* = 0.21
	Sham	10	24.02 ± 7.10	24.11 ± 5.67	+0.09 (0.93, 0.93, 0.01)		23.46 ± 7.54	-0.56 (0.64, 0.93, -0.07)	
P100 IT. 0.25º (ms)	**Anodal**	11	106.21 ± 2.44	106.58 ± 2.38	+0.36 (0.60, 0.72, 0.15)	*p* = 0.08 *q* = 0.24 *g* = 0.79	107.28 ± 2.48	+1.07 (0.14, 0.28, 0.42)	*p* = 0.22 *q* = 0.33 *g* = 0.55
	Sham	10	108.37 ± 2.51	107.16 ± 1.85	-1.22 (0.03, 0.20, -0.53)		108.13 ± 2.45	-0.24 (0.77, 0.77, -0.09	

Table 2. P100 amplitude and implicit time at 1º and 0.25º stimulus - Table entries report mean ± SD values for VEP parameters across visits: baseline (v0), after a single HD-tDCS session (v1), and after four sessions (v2). Changes from baseline (Δ) and associated statistics (p, FDR q-value within each VEP metric, and Hedges' g) assess acute (Δv1-v0) and cumulative (Δv2-v0) cortical responses to each associated stimulation condition. Between-group statistics compare the change in VEP responses from Anodal compared to Sham. Significance was set at q < 0.05.

5.3. Pattern Electroretinogram

P50 and N95 amplitudes and implicit times were analyzed for PERG. No acute or cumulative within-group changes in any PERG metric survived FDR correction (all q > 0.33). Between-group comparisons revealed no statistically significant differences for either acute or cumulative change in any PERG metric after FDR correction within each metric (all q > 0.26) (see table 3).

			Baseline	Visit 1			Visit 2		
	Group	n	v0 [mean ± SD]	v1 [mean ± SD]	Δ(v1-v0) (*p*, *q*, *g*)	Between group Δv1-v0	v2 [mean ± SD]	Δ(v2-v0) (*p*, *q*, *g*)	Between group Δv2-v0
P50 Amp. (µV)	Anodal	11	6.40 ± 1.53	6.08 ± 0.79	-0.31 (0.48, 0.92, -0.25)	*p* = 0.46 *q* = 0.92 *g* = -0.32	6.33 ± 1.33	-0.07 (0.92, 0.92, -0.05)	*p* = 0.75 *q* = 0.92 *g* = 0.12
	Sham	10	6.60 ± 1.31	6.70 ± 1.28	+0.10 (0.77, 0.92, 0.07)		6.22 ± 1.98	-0.38 (0.13, 0.92, -0.21)	
P50 IT. (ms)	Anodal	11	55.15 ± 1.61	55.65 ± 2.43	+0.50 (0.56, 0.90, 0.24)	*p* = 0.76 *q* = 0.90 *g* = 0.13	55.25 ± 2.12	+0.11 (0.90, 0.90, 0.06)	*p* = 0.59 *q* = 0.90 *g* = -0.23
	Sham	10	55.06 ± 1.84	55.21 ± 2.41	+0.16 (0.84, 0.90, 0.07)		55.82 ± 1.89	+0.77 (0.41, 0.90, 0.39)	
N95 Amp. (µV)	Anodal	11	11.20 ± 2.11	10.87 ± 2.21	-0.32 (0.52, 0.78, -0.14)	*p* = 0.92 *q* = 0.78 *g* = -0.05	12.86 ± 2.82	+1.67 (0.11, 0.33, 0.64)	*p* = 0.04 *q* = 0.26 *g* = 0.91
	Sham	10	11.50 ± 2.64	11.30 ± 2.18	-0.21 (0.84, 0.90, -0.08)		10.43 ± 2.37	-1.07 (0.22, 0.33, -0.41)	
N95 IT. (ms)	Anodal	11	93.06 ± 3.79	93.03 ± 4.95	-0.04 (0.99, 0.99, -0.01)	*p* = 0.80 *q* = 0.99 *g* = -0.10	92.65 ± 3.74	-0.41 (0.80, 0.99, -0.10)	*p* = 0.43 *q* = 0.99 *g* = -0.34
	Sham	10	93.56 ± 4.99	94.16 ± 2.84	+0.60 (0.71, 0.99, 0.14)		94.96 ± 4.84	+1.40 (0.41, 0.99, 0.27)	
N95/P50 Ratio (ms)	Anodal	11	1.80 ± 0.34	1.79 ± 0.28	-0.01 (0.88, 0.88, -0.04)	*p* = 0.65 *q* = 0.88 *g* = 0.20	2.06 ± 0.30	+0.25 (0.13, 0.66, 0.76)	*p* = 0.22 *q* = 0.66 *g* = 0.53
	Sham	10	1.80 ± 0.51	1.70 ± 0.25	-0.10 (0.54, 0.88, -0.23)		1.74 ± 0.34	-0.06 (0.77, 0.66, -0.13)	

Table 3. PERG outcomes including P50 and N95 wave amplitudes and implicit times - Table entries report mean ± SD values for PERG parameters across visits: baseline (v0), after a single HD-tDCS session (v1), and after four sessions (v2). Changes from baseline (Δ) and associated statistics (p, FDR q-value within each PERG metric, and Hedges' g) assess acute (Δv1-v0) and cumulative (Δv2-v0) retinal responses to each associated stimulation condition. Between-group statistics compare the change in PERG responses from Anodal compared to Sham. Significance was set at q < 0.05.

5.4. Best Corrected Visual Acuity

BCVA was analyzed by the number of letters the participants could see. Within the anodal group, BCVA showed a trend towards significance after four sessions (Δ = +2.14, p = 0.01, q = 0.07, g = 0.51), although this did not reach statistical significance after FDR correction. No other acute or cumulative within-group changes in BCVA reached statistical significance (all q > 0.07).

Between-group comparisons revealed no significant differences in acute or cumulative BCVA change (Δv1-v0: p = 0.36, q = 0.43, g = 0.39; Δv2-v0: p = 0.18, q = 0.31, g = 0.59) (see Table 4).

			Baseline	Visit 1			Visit 2		
	Group	**n**	**v0 [mean ± SD]**	**v1 [mean ± SD]**	**Δ(v1-v0) (*p, q, g*)**	**Between group Δv1-v0**	**v2 [mean ± SD]**	**Δ(v2-v0) (*p, q, g*)**	**Between group Δv2-v0**
BCVA (letters)	**Anodal**	11	50.64 (4.08)	51.50 (3.46)	+0.86 (0.20, 0.31, 0.22)	*p* = 0.36 *q* = 0.43 *g* = 0.49	52.77 (3.97)	+2.14 (0.01, 0.07, 0.51)	*p* = 0.18 *q* = 0.31 *g* = 0.59
	Sham	10	49.90 (2.20)	49.85 (3.74)	-0.05 (0.95, 0.95, -0.02)		50.75 (3.03)	-0.38 (0.18, 0.31, 0.31)	

Table 4. BCVA outcomes in number of letters seen - Table entries report mean ± SD values for BCVA parameters across visits: baseline (v0), after a single HD-tDCS session (v1), and after four sessions (v2). Changes from baseline (Δ) and associated statistics (p, FDR q-value within each BCVA metric, and Hedges' g) assess acute (Δv1-v0) and cumulative (Δv2-v0) visual acuity changes to each associated stimulation condition. Between-group statistics compare the change in BCVA responses from Anodal compared to Sham. Significance was set at q < 0.05.

5.5. Optical Coherence Tomography

Across all macular thickness regions (central 1mm, 3mm, and 6mm rings), peripapillary RNFL thickness sectors (temporal, superior, nasal, inferior and overall average), and macular GCL thickness subfields (superior, superotemporal, superonasal, inferonasal, inferior, inferotemporal and overall average), neither acute nor cumulative changes were statistically significant in either group after FDR correction.

5.6. Side-effects Questionnaire and Stimulation Perception

Across all sessions, the most frequently reported side effects were tingling and itching, which were predominantly observed in the anodal group (see Table 5 and Figure 5). Tingling was reported by up to 45% of participants in the anodal group and up to 20% in the sham group, with mean intensities rated as mild. Itching was reported by 36% in the anodal group and 30% in the sham group, again with mild intensity. Skin redness (20%) and sleepiness (9%) were only reported in the anodal group, and all cases were mild or moderate. No other side effects including headache, neck pain, scalp pain, burning, trouble concentrating, mood change, or other symptoms were reported in either group across all sessions. Statistical analysis using Fisher's Exact Test revealed no significant differences between groups for any side effect at any session (all p >0 .05)

Side Effect	Session 1		Session 2		Session 3		Session 4	
	Anodal	Sham	Anodal	Sham	Anodal	Sham	Anodal	Sham
Headache	0	0	0	0	0	0	0	0
Neck pain	0	0	0	0	0	0	0	0
Scalp pain	0	0	0	0	0	0	0	0
Tingling	5/11	2/10	4/11	1/10	3/11	1/10	4/11	1/10
Itching	4/11	3/10	3/11	2/10	3/11	1/10	3/11	2/10
Burning	0	0	0	0	0	0	0	0
Skin redness	2/11	0	2/11	0	2/11	0	3/11	0
Sleepiness	1/11	0	0	0	0	0	1/11	0
Trouble concentrating	0	0	0	0	0	0	0	0
Mood change	0	0	0	0	0	0	0	0
Others	0	0	0	0	0	0	0	0

Table 5. Number of participants reporting HD-tDCS side effects. Values indicate the number of subjects reporting each side effect out of the total number in each group (anodal: n=11; sham: n=10) for each session.

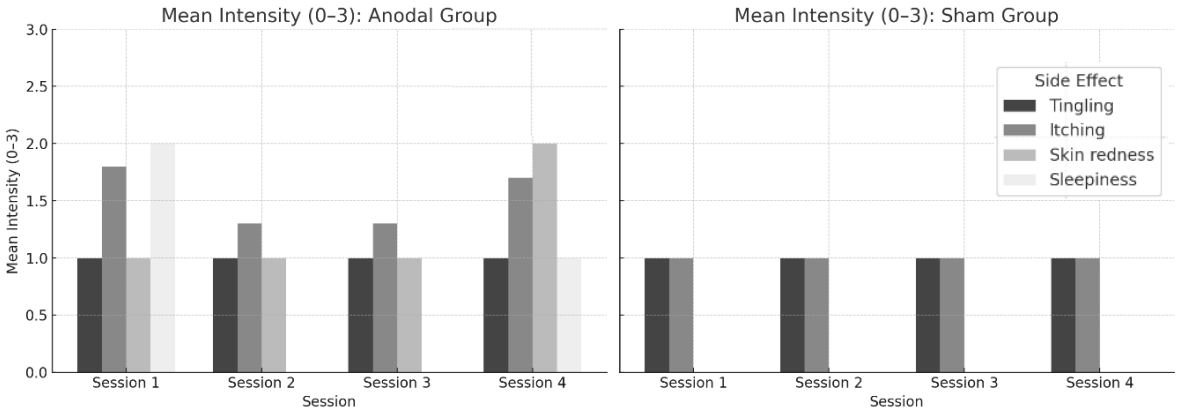

Figure 5. Mean intensity of the most frequently reported side effects (0-3; 0 = no sensation; 1 = mild; 2 = moderate; 3 = severe) in the anodal (left) and sham (right) groups across four consecutive sessions of HD-tDCS. Bars represent the average intensity reported by participants who experienced tingling, itching, skin redness, or sleepiness during each session.

The effectiveness of blinding was assessed by asking participants to guess whether they had received active or sham stimulation after each session. As shown in Table 6, across all four sessions, both anodal and sham groups exhibited similar patterns of guesses, with no consistent ability to correctly identify the stimulation condition. For example, in the anodal group, between 54.5% and 72.7% of participants guessed they had received active stimulation across sessions, while in the sham group, this proportion ranged from 70.0% to 80.0%.

Fisher's Exact Test revealed no statistically significant association between the actual stimulation condition and the participant's guess in any session (all p-values > 0.05). The odds ratios for correctly identifying the stimulation condition were 0.51, 0.75, 0.75, and 0.67 for sessions 1 through 4, respectively, further indicating that the odds of guessing "active" were similar between groups and that blinding was effective.

	Session 1		**Session 2**		**Session 3**		**Session 4**	
	Said Active	**Said Sham**	**Said Active**	**Said Sham**	**Said Active**	**Said Sham**	**Said Active**	**Said Sham**
Active(n=11)	6 (54.5%)	5 (45.5%)	7 (63.6%)	4 (36.4%)	7 (63.6%)	4 (36.4%)	8 (72.7%)	3 (27.3%)
Sham(n=10)	7 (70.0%)	3 (30.0%)	7 (70.0%)	3 (30.0%)	7 (70.0%)	3 (30.0%)	8 (80.0%)	2 (20.0%)
Fisher's p-value	0.659		1.000		1.000		1.000	
Odds Ratio	0.51		0.75		0.75		0.67	

Table 6. Participants' guesses regarding stimulation condition by session and actual group. Fisher's Exact Test p-values and odds ratios are reported for each session

6. Discussion

6. Discussion

In this study, we conducted the first multimodal assessment of the effects of anodal HD-tDCS over the primary visual cortex on multiple visual and cortical measures in a healthy adult sample. Our findings provide evidence of subtle improvements in contrast sensitivity and enhanced functional integrity of the visual pathway.

Improvements of anodal HD-tDCS over V1 on Contrast Sensitivity

Anodal HD-tDCS over V1 produced significant improvements in CS at several mid-to-high spatial frequencies. Improvements were evident even after a single session at 3.4 cpd and became stronger and broader across frequencies after four sessions particularly at 2.2, 3.4, 7.1, and 14.2 cpd, with moderate to large effect sizes. The sham group showed only minimal, non-significant practice related gains. These findings indicate that anodal HD-tDCS can acutely sharpen contrast perception and further augment it with repeated exposure, at least for spatial frequencies that engage mid-level detail and finer pattern detection. Interestingly, no significant changes were seen at the lowest frequencies (0.55 and 1.1 cpd), possibly because very coarse stimulus were already near ceiling performance (little room for improvement) or involve visual channels less susceptible to tDCS modulation (Behrens et al., 2017; Bello et al., 2023; Reinhart et al., 2016; Richard et al., 2015).

These results are consistent with studies showing that anodal stimulation of visual cortex enhances contrast sensitivity, likely by lowering contrast detection thresholds through increased cortical excitability. Results from Bello et al. (2023) meta-analyses showed beneficial acute effects of tES in enhancing contrast sensitivity. Additionally, Behrens et al. (2017) demonstrated that with repetitive stimulation, anodal tDCS significantly improved contrast sensitivity in central vision, even after 4 weeks after the last stimulation.

It is important to note that the spatial frequencies benefiting most (around 2-7 cpd) correspond to mid-range detail processing, which might recruit neurons in V1 that were optimally modulated by the stimulation. Higher frequency (such as 14.2 cpd) improvement suggests even fine detail detection can be enhanced, although this was evident only after repeated sessions, implying an effect buildup for the highest acuity

demands. In fact, in the primary visual cortex, neurons near the apex of the calcarine sulcus prefer higher spatial frequencies and lie closer to the cortical surface, where tDCS-induced electric fields are strongest. Therefore, tDCS effects on contrast sensitivity may be most pronounced with more mid to high spatial frequency gratings (Reinhart et al., 2016; Richard et al., 2015). Our findings support these results by showing a robust facilitation of contrast processing under anodal HD-tDCS, and extend them by using an HD strategy, which delivers more focal currents. The focality of HD-tDCS may enhance neuromodulation at the cortical representation of the tested stimulus, as current density peaks at the visual cortical apex (retinotopically mapped to central vision, where contrast sensitivity is highest) potentially explaining the frequency-specific gains observed (Behrens et al., 2017; Himmelberg et al., 2022; Kuo et al., 2013).

Anodal HD-tDCS over V1 is believed to enhance cortical excitability by inducing subthreshold depolarization of neuronal membranes, thereby increasing the responsiveness of visual neurons. This neuromodulatory effect shifts the contrast response function, making weak visual inputs more likely to elicit neuronal firing and improving behavioral sensitivity to low-contrast stimuli. Additionally, repeated stimulation is thought to engage synaptic plasticity mechanisms analogous to LTP and may influence local neurochemical balance by reducing inhibitory GABAergic transmission (Behrens et al., 2017). tDCS effects also resemble natural learning processes in the visual cortex, which involve NMDA receptor activation and increased BDNF (Brain Derived Neurotrophic Factor) levels (Fritsch et al., 2010; Kim et al., 2010). These mechanisms support synaptic strengthening and the consolidation of visual learning, aligning with existing models of tDCS-induced plasticity in sensory cortices (Behrens et al., 2017).

An improved cortical signal-to-noise ratio may also contribute, either by suppressing intrinsic neural noise or by altering functional connectivity patterns, making target gratings more salient relative to background activity. Notably, some evidence points to polarity-specific effects: anodal stimulation typically facilitates performance in tasks involving contrast or visual acuity, while cathodal stimulation (which hyperpolarizes cortical neurons) can impair contrast sensitivity or, paradoxically, improve tasks like motion discrimination by reducing cortical noise (Behrens et al., 2017; Reinhart et al., 2016; Stagg et al., 2009).

In the present study, only anodal stimulation was applied, and the observed improvements in contrast sensitivity are consistent with the expected excitatory effects. The lack of change at lower spatial frequencies (e.g., 0.55 and 1.1 cpd) suggests that tDCS does not uniformly affect all visual pathways. Processing of low spatial frequencies may require different stimulation parameters or may already operate near optimal efficiency in healthy individuals (Behrens et al., 2017; Bello et al., 2023; Reinhart et al., 2016; Richard et al., 2015).

While some prior studies have reported modest improvements in contrast sensitivity following anodal tDCS to the primary visual cortex, these effects are typically small, variable, and often transient. Evidence also suggests that learning, initial performance, practice effects, as well as inter-individual variability, can overshadow or mimic the effects of stimulation, limiting the achievement of more significant results (He et al., 2019; Wu et al., 2021). Furthermore, while there was an attempt to reduce learning effect bias by repeating the baseline measures three times, the improvement in all spatial frequencies from both groups was noted, meaning that the baseline measures might have benefited from extra trials to reduce this learning effect. Despite this, the fact that Anodal had more withing group changes from baseline and between groups a more trending increase in the Anodal group from baseline to Visit 2 suggests that the effects in cortical excitability may bypass this learning bias and trend to prove actual effects of HD-tDCS on CS.

No robust modulation of VEP P100 following Anodal HD-tDCS, despite subtle trends

No significant changes were observed in the VEP P100 waveform - neither in amplitude nor implicit time - following anodal HD-tDCS, whether acutely or cumulatively. The P100 component, which is primarily generated in V1, serves as a well-established marker of cortical excitability and the functional integrity of the visual pathway (Odom et al., 2016). We hypothesized that anodal stimulation would increase P100 amplitude, based on prior studies reporting enhanced VEP amplitudes following occipital tES (Antal et al., 2004; Bello et al., 2023) . In our data, P100 amplitudes in the anodal group did show a small increase (on average 1-2 μV) relative to baseline, and the effect size for the cumulative change was large (Hedges' $g > 1$ at the 1º stimulus size), but high inter-subject

variability and conservative statistical correction meant this did not reach significance. The sham group showed no systematic changes. Thus, while there was a trend of anodal HD-tDCS increasing VEP amplitude, we cannot conclusively confirm this effect. Notably, our between-group comparison for cumulative P100 amplitude change approached significance (uncorrected p= 0.02), suggesting that with a larger sample or slightly more sessions, a reliable VEP enhancement might have been detected.

Contextualizing our VEP findings by prior research, some studies have indeed found anodal tDCS increases pattern-reversal VEP amplitudes, consistent with an excitability boost (Ding et al., 2016; Dong et al., 2020; Lau et al., 2021; Nakazono et al., 2020). For example, Melnick et al. (2016) reported enhanced steady-state VEP amplitudes with occipital anodal stimulation, and Accornero et al. (2017) noted increased P100 amplitude immediately after tDCS in migraine patients. However, others have failed to observe significant VEP changes in healthy subjects or found only subtle modulation of VEP habituation rather than amplitude. Our results fall somewhere in between, hinting at a positive effect that did not reach significance. Methodological factors may explain the discrepancy: our VEPs were recorded approximately 30 minutes post-stimulation, capturing offline aftereffects. It's possible that the strongest excitability changes occur during or immediately after stimulation (online effects) (He et al., 2019; Wu et al., 2021).

Preserved retinal ganglion cell function following occipital HD-tDCS

We found no changes in PERG P50 or N95 waves after HD-tDCS, indicating that macular and retinal ganglion cell functions were unaffected by occipital stimulation. The PERG reflects activity originating largely from the RGCs in the retina (P50 and N95 components correspond to different phases of RGC light response) (Thompson et al., 2024). Since our stimulation targeted V1 in the occipital cortex, it is not surprising that no strong effect was observed at the retinal level (Potok et al., 2023). While stimulation of V1, such as with anodal HD-tDCS, can enhance cortical responses like the P100 component of the VEP, there is no evidence in humans that it directly increases the N95 component of the PERG in healthy individuals (Potok et al., 2023; Strang et al., 2018). These two electrophysiological signals originate from distinct stages of the visual pathway: the N95 reflects retinal ganglion cell activity, whereas the P100 arises from cortical processing in the primary visual cortex. They are functionally sequential, not bidirectionally coupled,

although under certain pathological conditions, cortical feedback mechanisms or disinhibition might indirectly influence pre-cortical structures (Holder, 2002; Marmoy & Viswanathan, 2021; Perin et al., 2020).

No significant gains in high-contrast VA after anodal HD-tDCS

BCVA testing found no statistically significant improvement in high contrast visual acuity (measured as letter recognition) after either one or four sessions of anodal HD-tDCS. There was a small positive shift in acuity in the anodal group after four sessions (on average +2 letters), but this did not survive multiple-comparison corrections and was not significantly different from sham changes. This suggests that anodal HD-tDCS did not meaningfully enhance maximum visual resolution in young adults with normal vision.

One likely explanation is the ceiling effect since the participants had near-optimal acuity at baseline (approximately 20/20 or better), leaving little room for measurable improvement. Unlike contrast sensitivity (which tests near-threshold vision and can reveal subtle gains in sensitivity), high-contrast acuity is a suprathreshold task where performance is already saturated in healthy eyes. Thus, modulating cortical excitability may not further improve letter acuity when it is at peak levels pre-stimulation. In the literature, tDCS effects on visual acuity are not well-documented, however, literature has reported improvements in visual functions including acuity and contrast sensitivity with visual cortex stimulation (Reinhart et al., 2016). On the other end the review from Bello et al. (2023) stated no improvements in healthy subjects VA, highlighting the dichotomy of the findings.

No effects of anodal HD-tDCS on retinal structure

No structural changes were detected in the retina or optic nerve after HD-tDCS. Optical Coherence Tomography was used to measure macular thickness, macular volume, peripapillary retinal nerve fiber layer thickness, and macular ganglion cell layer thickness. All these metrics remained stable from baseline through post-stimulation follow-ups, with no significant differences between anodal and sham groups. This outcome was anticipated since there was no scientific evidence explaining short-term neuromodulation would not be expected to induce anatomical changes in retinal tissue. The integrity of retinal layers

over the course of the experiment confirms the HD-tDCS non-invasive nature that does not cause retinal or optic nerve edema, swelling, or neurodegenerative changes, at least within the timeframe and stimulation parameters of our study.

Acute versus cumulative effects of anodal HD-tDCS on visual and cortical outcomes

In order to address whether the effects of HD-tDCS differ between a single session and multiple sessions, we compared outcomes at baseline, after one stimulation, and after four cumulative stimulations. Our findings indicate that repeated HD-tDCS sessions led to greater and more widespread visual enhancements than a single session, supporting the idea of cumulative neuroplasticity-like enhancement.

After one session of anodal HD-tDCS, we observed a modest improvement in contrast sensitivity (significant at 3.4 cpd), but no significant changes in other measures. This suggests that even a single 20 minute session can induce a short-term boost in certain aspects of visual perception likely reflecting early aftereffects of tDCS on cortical excitability. The presence of an acute CS improvement aligns with reports that even one occipital tDCS session can alter visual processing from minutes to hours afterward. However, the limited scope of acute changes (one spatial frequency improved) in our study also underlines that a single session might produce only subtle benefits in a healthy, high-performing visual system (Behrens et al., 2017; Bello et al., 2023; Reinhart et al., 2016).

After four consecutive HD-tDCS sessions, the improvements in contrast sensitivity became more robust and extended to multiple spatial frequencies as discussed above. We also saw that only with repeated sessions did some outcomes show hints of change, for example VEP P100 amplitude increases were most evident cumulatively (though not significant). This pattern implies that repetition promotes consolidation of tDCS-induced changes (Behrens et al., 2017). Each session may induce transient physiological changes, and when sessions are repeated, these changes can accumulate or interact to produce stronger effects. Our results thus support the hypothesis that repeated tDCS drives longer lasting and stronger neuronal modifications than a single exposure (Behrens et al., 2017; Ding et al., 2016; Nakazono et al., 2020). This is in line with literature observations that repeated visual cortex stimulation exerts cumulative influences, potentially consolidating

learning-like effects through sustained synaptic remodeling (Olma et al., 2013; Kim et al., 2016).

It is important to note that in our study design, all post-stimulation assessments were conducted within 2 hours immediately after the HD-tDCS sessions. Therefore, we demonstrated cumulative short-term aftereffects, but we did not assess long-term retention beyond the stimulation day. Other studies showed improved motion perception lasting days after five sessions proving that serial tDCS sessions can lead to effects that persist for days or weeks if measurements are taken later, indicating genuine long-term plasticity-like effects (Behrens et al., 2017; Bello et al., 2023; Olma et al., 2013). While we did not test beyond the final session, the fact that performance improvements grew over consecutive days hints that some longer-lasting neural changes were taking place. Repeated anodal stimulation might be engaging mechanisms like LTP-like increases in synaptic efficacy or changes in cortical inhibitory/excitatory balance that outlast each daily session (Antal et al., 2011; Behrens et al., 2017; Kuo et al., 2013). Future work with follow-up testing will be needed to determine how stable these gains are.

By comparing anodal vs. sham changes, we attribute the larger improvements to the stimulation rather than just learning or familiarization with the tasks. This controlled design strengthens the conclusion that HD-tDCS actively induced neuroplastic changes rather than participants simply improving with practice.

HD-tDCS safety, tolerability and blinding

This study involved the application of a low-intensity electrical current to the scalp over the occipital cortex, and it is good practice to adhere to assess the safety, tolerability and blinding in this type of studies. Existing literature on both conventional tDCS and HD-tDCS indicates that these protocols are generally well-tolerated and considered safe. Reported side effects are typically mild and transient, such as itching, tingling sensations, mild headache, redness, and a burning sensation at the stimulation site (Brunoni et al., 2011; Fertonani et al., 2015; Reckow et al., 2018). A comprehensive review by Bikson et al. (2016), which analyzed data from over 33,000 transcranial electrical stimulation sessions, found no evidence of serious adverse events, thereby reinforcing the favorable safety profile of tDCS. In line with these findings, the current study observed a similar safety and tolerability profile, with the most commonly reported side effects (tingling and

itching) being mild, transient, and only slightly more prevalent in the active stimulation group. No serious or unexpected adverse events were reported, further supporting the safety of HD-tDCS under the parameters used.

In addition to safety, the effectiveness of blinding is an important consideration in non-invasive brain stimulation research in order to prevent expectancy bias. Previous studies have demonstrated that participants in both active and sham (placebo) conditions are generally unable to distinguish which type of stimulation they received, with sensory experiences reported in sham HD-tDCS closely resembling those of active stimulation and resulting in comparable sensation profiles (Reckow et al., 2018). Notably, participants are equally likely to believe they received active stimulation, regardless of the actual condition administered or the stimulation intensity used in the study. Consistently non-significant results across all sessions in the present study demonstrate robust blinding, with participants' ability to guess the stimulation condition remaining at chance level regardless of session number. These findings confirm that participants were unable to reliably distinguish between active and sham HD-tDCS, aligning with prior literature and supporting the effectiveness of the blinding procedures implemented (Reckow et al., 2018).

7. Limitations

7. Limitations

When interpreting our results, some limitations need acknowledgement. First, the sample size was modest (approximately 10-11 participants per group), which, despite being common in neurostimulation experiments, may limit statistical power especially for subtle effects.

Our stimulation protocol and outcome tests were fixed in order and timing. According to Kuo et al. (2013), anodal HD-tDCS induces offline excitability changes with a delayed peak at approximately 30 minutes post-stimulation, followed by a gradual return to baseline within 6 hours. Since no measurements were conducted beyond the 2 hour mark and within a time frame shown to reliably capture the after-effects of stimulation, we had a safe time window to take all post-stimulation measures. However, it is possible that measurements taken later within this window may have shown reduced effects, as they no longer aligned with the peak of stimulation-induced excitability (Kuo et al., 2013).

Additionally, although baseline CS measurements were repeated three times to minimize learning effects, improvements were still observed in both groups. This indicates that the baseline data may have been influenced by practice effects, and that including additional trials could have further reduced this bias.

8. Future Directions

8. Future Directions

Our results attribute CS and cortical function improvements to neurophysiological mechanisms, but these statements remain inferential. Since we are attributing it to increased cortical excitability and potential LTP-like synaptic potentiation and although consistent with animal studies and human indirect measures, we did not directly measure cortical neurotransmitter levels or synaptic changes. Incorporating techniques like magnetic resonance spectroscopy (for GABA/glutamate changes) or functional MRI could elucidate how HD-tDCS rebalances cortical networks. Future studies could incorporate real-time EEG or imaging during and after HD-tDCS to better understand neural changes. For instance, measuring changes in oscillatory activity or connectivity (via EEG/MEG or fMRI) could reveal whether HD-tDCS is enhancing functional communication within visual cortex or between V1 and higher areas. Likewise, assessing changes in cortical inhibition/excitation balance (using MRS or paired pulse TMS techniques) could directly test the hypothesis of a shift toward greater cortical excitability or neurochemical changes underlying the behavioral improvements.

While our results in healthy adults set a baseline, individuals with visual cortex damage or neuro-ophthalmological diseases might respond differently to tDCS. Healthy neural networks might exhibit homeostatic plasticity that limits the magnitude of tDCS effects (to maintain equilibrium), whereas in cases of injury or abnormal visual development, the cortex might be more susceptible or responsive to modulation. Therefore, a logical future direction is to test HD-tDCS in specific clinical contexts, for example, in amblyopia (to see if contrast sensitivity and acuity in the weaker eye can be improved), or in post-stroke hemianopia rehabilitation (to engage plasticity in spared V1 or extrastriate areas). Some preliminary studies and case reports suggest tDCS can assist visual rehabilitation in patients, but more rigorous trials are needed.

9. Conclusion

9. Conclusion

This study offers evidence that anodal HD-tDCS applied over the primary visual cortex can enhance visual function in healthy adults, as assessed through a multimodal visual and cortical approach. The observed improvements in CS at mid-to-high spatial frequencies following both single and repeated stimulation sessions suggest that anodal HD-tDCS is capable of modulating perceptual thresholds by augmenting cortical excitability in a focal and reproducible manner. These findings are consistent with prior literature reporting conventional tDCS-induced enhancements in visual perception and further extend existing knowledge by employing a focal 4×1 montage and a cumulative stimulation protocol over multiple sessions.

Electrophysiological data reinforces the functional findings as there was a close to significance increase in the amplitude of the P100 component of VEP stimulation suggesting enhanced visual cortical responsiveness, potentially attributable to increased excitatory synaptic activity or improved neuronal synchrony within early visual areas. However, no significant changes were observed in the P50 and N95 components of the PERG, indicating that macular and retinal ganglion cell function remained stable. This dissociation supports the view that although VEP and PERG represent sequential processing stages along the visual pathway, they may be independently modulated under conditions of non-invasive cortical stimulation in healthy individuals. Structural retinal and optic nerve measures, as assessed through OCT, revealed no measurable alterations in macular GCL and retinal thickness or peripapillary RNFL following stimulation, providing confirmation that cortical interventions do not elicit adverse retinal neuronal layers consequences.

By integrating psychophysical, electrophysiological, and structural methodologies, the present study contributes a comprehensive characterization of HD-tDCS-induced modulation within the visual system. These findings offer mechanistic information into the neurophysiological effects of focal cortical stimulation and establish a reference for the future application of HD-tDCS in clinical populations. Continued investigation is needed to assess the longevity of these effects, explore dose-response relationships, and examine potential therapeutic benefits in visual disorders characterized by cortical hypoexcitability or altered visual processing.

10. References

10. References

Aberra, A. S., Wang, R., Grill, W. M., & Peterchev, A. V. (2023). Multi-scale model of axonal and dendritic polarization by transcranial direct current stimulation in realistic head geometry. *Brain Stimulation*, *16*(6), 1776–1791. https://doi.org/10.1016/j.brs.2023.11.018

Alam, M., Truong, D. Q., Khadka, N., & Bikson, M. (2016). Spatial and polarity precision of concentric high-definition transcranial direct current stimulation (HD-tDCS). *Physics in Medicine and Biology*, *61*(12), 4506–4521. https://doi.org/10.1088/0031-9155/61/12/4506

Antal, A., Kincses, T. Z., Nitsche, M. A., Bartfai, O., & Paulus, W. (2004a). Excitability Changes Induced in the Human Primary Visual Cortex by Transcranial Direct Current Stimulation: Direct Electrophysiological Evidence. *Investigative Ophthalmology and Visual Science*, *45*(2), 702–707. https://doi.org/10.1167/iovs.03-0688

Antal, A., Kincses, T. Z., Nitsche, M. A., Bartfai, O., & Paulus, W. (2004b). Excitability Changes Induced in the Human Primary Visual Cortex by Transcranial Direct Current Stimulation: Direct Electrophysiological Evidence. *Investigative Ophthalmology and Visual Science*, *45*(2), 702–707. https://doi.org/10.1167/iovs.03-0688

Antal, A., Luber, B., Brem, A. K., Bikson, M., Brunoni, A. R., Cohen Kadosh, R., Dubljević, V., Fecteau, S., Ferreri, F., Flöel, A., Hallett, M., Hamilton, R. H., Herrmann, C. S., Lavidor, M., Loo, C., Lustenberger, C., Machado, S., Miniussi, C., Moliadze, V., … Paulus, W. (2022). Non-invasive brain stimulation and neuroenhancement. In *Clinical Neurophysiology Practice* (Vol. 7, pp. 146–165). Elsevier B.V. https://doi.org/10.1016/j.cnp.2022.05.002

Antal, A., Nitsche, M. A., & Paulus, W. (2006). Transcranial direct current stimulation and the visual cortex. *Brain Research Bulletin*, *68*(6), 459–463. https://doi.org/10.1016/j.brainresbull.2005.10.006

Antal, A., Paulus, W., & Nitsche, M. A. (2011). Electrical stimulation and visual network plasticity. In *Restorative Neurology and Neuroscience* (Vol. 29, Issue 6, pp. 365–374). https://doi.org/10.3233/RNN-2011-0609

Arif, Y., Embury, C. M., Spooner, R. K., Okelberry, H. J., Willett, M. P., Eastman, J. A., & Wilson, T. W. (2022a). High-definition transcranial direct current stimulation of the occipital cortices induces polarity dependent effects within the brain regions serving attentional reorientation. *Human Brain Mapping*, *43*(6), 1930–1940. https://doi.org/10.1002/hbm.25764

Arif, Y., Embury, C. M., Spooner, R. K., Okelberry, H. J., Willett, M. P., Eastman, J. A., & Wilson, T. W. (2022b). High-definition transcranial direct current stimulation of the occipital cortices

induces polarity dependent effects within the brain regions serving attentional reorientation. *Human Brain Mapping*, *43*(6), 1930–1940. https://doi.org/10.1002/hbm.25764

Behrens, J. R., Kraft, A., Irlbacher, K., Gerhardt, H., Olma, M. C., & Brandt, S. A. (2017). Long-lasting enhancement of visual perception with repetitive noninvasive transcranial direct current stimulation. Frontiers in Cellular Neuroscience, 11. https://doi.org/10.3389/fncel.2017.00238

Bear, M., Connors, B., & Paradiso, M. A. (2020). Neuroscience: Exploring the Brain, Enhanced Edition: Exploring the Brain, Enhanced Edition. Jones & Bartlett Learning.

Bello, U. M., Wang, J., Park, A. S. Y., Tan, K. W. S., Cheung, B. W. S., Thompson, B., & Cheong, A. M. Y. (2023a). Can visual cortex non-invasive brain stimulation improve normal visual function? A systematic review and meta-analysis. In *Frontiers in Neuroscience* (Vol. 17). Frontiers Media SA. https://doi.org/10.3389/fnins.2023.1119200

Bello, U. M., Wang, J., Park, A. S. Y., Tan, K. W. S., Cheung, B. W. S., Thompson, B., & Cheong, A. M. Y. (2023b). Can visual cortex non-invasive brain stimulation improve normal visual function? A systematic review and meta-analysis. In *Frontiers in Neuroscience* (Vol. 17). Frontiers Media SA. https://doi.org/10.3389/fnins.2023.1119200

Bhattacharya, A., Mrudula, K., Sreepada, S. S., Sathyaprabha, T. N., Pal, P. K., Chen, R., & Udupa, K. (2022). An Overview of Noninvasive Brain Stimulation: Basic Principles and Clinical Applications. In *Canadian Journal of Neurological Sciences* (Vol. 49, Issue 4, pp. 479–492). Cambridge University Press. https://doi.org/10.1017/cjn.2021.158

Bikson, M., Grossman, P., Thomas, C., Zannou, A. L., Jiang, J., Adnan, T., Mourdoukoutas, A. P., Kronberg, G., Truong, D., Boggio, P., Brunoni, A. R., Charvet, L., Fregni, F., Fritsch, B., Gillick, B., Hamilton, R. H., Hampstead, B. M., Jankord, R., Kirton, A., … Woods, A. J. (2016). Safety of Transcranial Direct Current Stimulation: Evidence Based Update 2016. In *Brain Stimulation* (Vol. 9, Issue 5, pp. 641–661). Elsevier Inc. https://doi.org/10.1016/j.brs.2016.06.004

Brunoni, A. R., Amadera, J., Berbel, B., Volz, M. S., Rizzerio, B. G., & Fregni, F. (2011). A systematic review on reporting and assessment of adverse effects associated with transcranial direct current stimulation. In *International Journal of Neuropsychopharmacology* (Vol. 14, Issue 8, pp. 1133–1145). https://doi.org/10.1017/S1461145710001690

Castaldi, E., Lunghi, C., & Morrone, M. C. (2020). Neuroplasticity in adult human visual cortex. In *Neuroscience and Biobehavioral Reviews* (Vol. 112, pp. 542–552). Elsevier Ltd. https://doi.org/10.1016/j.neubiorev.2020.02.028

Chen, L., Chen, G., Gong, X., & Fang, F. (2023). Integrating electric field modeling and pre-tDCS behavioral performance to predict the individual tDCS effect on visual crowding. *Journal of Neural Engineering*, *20*(5). https://doi.org/10.1088/1741-2552/acfa8c

Dayan, E., Censor, N., Buch, E. R., Sandrini, M., & Cohen, L. G. (2013). Noninvasive brain stimulation: From physiology to network dynamics and back. In *Nature Neuroscience* (Vol. 16, Issue 7, pp. 838–844). https://doi.org/10.1038/nn.3422

de Venecia, A. B. F., & Fresnoza, S. M. (2021). Visual cortex transcranial direct current stimulation for proliferative diabetic retinopathy patients: A double-blinded randomized exploratory trial. *Brain Sciences*, *11*(2), 1–17. https://doi.org/10.3390/brainsci11020270

Ding, Z., Li, J., Spiegel, D. P., Chen, Z., Chan, L., Luo, G., Yuan, J., Deng, D., Yu, M., & Thompson, B. (2016). The effect of transcranial direct current stimulation on contrast sensitivity and visual evoked potential amplitude in adults with amblyopia. *Scientific Reports*, *6*. https://doi.org/10.1038/srep19280

Dong, G., Wang, Y., & Chen, X. (2020). Anodal occipital tDCS enhances spontaneous alpha activity. *Neuroscience Letters*, *721*. https://doi.org/10.1016/j.neulet.2020.134796

Duménieu, M., Marquèze-Pouey, B., Russier, M., & Debanne, D. (2021). Mechanisms of plasticity in subcortical visual areas. In *Cells* (Vol. 10, Issue 11). MDPI. https://doi.org/10.3390/cells10113162

Fertonani, A., Ferrari, C., & Miniussi, C. (2015). What do you feel if I apply transcranial electric stimulation? Safety, sensations and secondary induced effects. *Clinical Neurophysiology*, *126*(11), 2181–2188. https://doi.org/10.1016/j.clinph.2015.03.015

Frase, L., Mertens, L., Krahl, A., Bhatia, K., Feige, B., Heinrich, S. P., Vestring, S., Nissen, C., Domschke, K., Bach, M., & Normann, C. (2021). Transcranial direct current stimulation induces long-term potentiation-like plasticity in the human visual cortex. *Translational Psychiatry*, *11*(1). https://doi.org/10.1038/s41398-020-01134-4

Fritsch, B., Reis, J., Martinowich, K., Schambra, H. M., Ji, Y., Cohen, L. G., & Lu, B. (2010). Direct current stimulation promotes BDNF-dependent synaptic plasticity: Potential implications for motor learning. *Neuron*, *66*(2), 198–204. https://doi.org/10.1016/j.neuron.2010.03.035

Hampstead, B. M., Mascaro, N., Schlaefflin, S., Bhaumik, A., Laing, J., Peltier, S., & Martis, B. (2020). Variable symptomatic and neurophysiologic response to HD-tDCS in a case series with posttraumatic stress disorder. *International Journal of Psychophysiology*, *154*, 93–100. https://doi.org/10.1016/j.ijpsycho.2019.10.017

He, Q., Lin, B. R., Zhao, J., Shi, Y. Z., Yan, F. F., & Huang, C. B. (2019). No effects of anodal transcranial direct current stimulation on contrast sensitivity function. *Restorative Neurology and Neuroscience*, *37*(2), 109–118. https://doi.org/10.3233/RNN-180881

Himmelberg, M. M., Winawer, J., & Carrasco, M. (2022). Linking individual differences in human primary visual cortex to contrast sensitivity around the visual field. *Nature Communications*, *13*(1). https://doi.org/10.1038/s41467-022-31041-9

Holder, G. E. (2002). *Pattern Electroretinography (PERG) and an Integrated Approach to Visual Pathway Diagnosis*.

Hooks, B. M., & Chen, C. (2007). Critical periods in the visual system: changing views for a model of experience-dependent plasticity. In *Neuron* (Vol. 56, Issue 2, pp. 312–326). https://doi.org/10.1016/j.neuron.2007.10.003

Kandel, E. R., Koester, J., Mack, S., & Siegelbaum, S. (2021). Principles of Neural Science, Fifth Edition. McGraw Hill Professional.

Karabanov, A., Ziemann, U., Hamada, M., George, M. S., Quartarone, A., Classen, J., Massimini, M., Rothwell, J., & Siebner, H. R. (2015). Consensus paper: Probing homeostatic plasticity of human cortex with non-invasive transcranial brain stimulation. In *Brain Stimulation* (Vol. 8, Issue 3, pp. 442–454). Elsevier Inc. https://doi.org/10.1016/j.brs.2015.01.404

Kim, S. J., Kim, B. K., Ko, Y. J., Bang, M. S., Kim, M. H., & Han, T. R. (2010). Functional and histologic changes after repeated transcranial direct current stimulation in rat stroke model. *Journal of Korean Medical Science*, *25*(10), 1499–1505. https://doi.org/10.3346/jkms.2010.25.10.1499

Kuo, H. I., Bikson, M., Datta, A., Minhas, P., Paulus, W., Kuo, M. F., & Nitsche, M. A. (2013). Comparing cortical plasticity induced by conventional and high-definition 4 × 1 ring tDCS: A neurophysiological study. *Brain Stimulation*, *6*(4), 644–648. https://doi.org/10.1016/j.brs.2012.09.010

Lau, C. I., Tseng, L. Y., Walsh, V., & Hsu, T. Y. (2021). Revisiting the effects of transcranial direct current stimulation on pattern-reversal visual evoked potentials. *Neuroscience Letters*, *756*. https://doi.org/10.1016/j.neulet.2021.135983

Liu, A., Vöröslakos, M., Kronberg, G., Henin, S., Krause, M. R., Huang, Y., Opitz, A., Mehta, A., Pack, C. C., Krekelberg, B., Berényi, A., Parra, L. C., Melloni, L., Devinsky, O., & Buzsáki, G. (2018). Immediate neurophysiological effects of transcranial electrical stimulation. In *Nature Communications* (Vol. 9, Issue 1). Nature Publishing Group. https://doi.org/10.1038/s41467-018-07233-7

Marmoy, O. R., & Viswanathan, S. (2021). Clinical electrophysiology of the optic nerve and retinal ganglion cells. In *Eye (Basingstoke)* (Vol. 35, Issue 9, pp. 2386–2405). Springer Nature. https://doi.org/10.1038/s41433-021-01614-x

Mattioli, F., Maglianella, V., D'Antonio, S., Trimarco, E., & Caligiore, D. (2024). Non-invasive brain stimulation for patients and healthy subjects: Current challenges and future perspectives. In *Journal of the Neurological Sciences* (Vol. 456). Elsevier B.V. https://doi.org/10.1016/j.jns.2023.122825

Müller, D., Habel, U., Brodkin, E. S., Clemens, B., & Weidler, C. (2023). HD-tDCS induced changes in resting-state functional connectivity: Insights from EF modeling. *Brain Stimulation*, *16*(6), 1722–1732. https://doi.org/10.1016/j.brs.2023.11.012

Nakazono, H., Ogata, K., Takeda, A., Yamada, E., Kimura, T., & Tobimatsu, S. (2020). Transcranial alternating current stimulation of α but not β frequency sharpens multiple visual functions. *Brain Stimulation*, *13*(2), 343–352. https://doi.org/10.1016/j.brs.2019.10.022

Odom, J. V., Bach, M., Brigell, M., Holder, G. E., McCulloch, D. L., Mizota, A., & Tormene, A. P. (2016). ISCEV standard for clinical visual evoked potentials: (2016 update). *Documenta Ophthalmologica*, *133*(1), 1–9. https://doi.org/10.1007/s10633-016-9553-y

Olma, M. C., Dargie, R. A., Behrens, J. R., Kraft, A., Irlbacher, K., Fahle, M., & Brandt, S. A. (2013). Long-term effects of serial anodal tDCS on motion perception in subjects with occipital stroke measured in the unaffected visual hemifield. *Frontiers in Human Neuroscience*, *JUN*. https://doi.org/10.3389/fnhum.2013.00314

Pereira, H. C., Sousa, D., Simões, M., Martins, R., Amaral, C., Lopes, V., Crisóstomo, J., & Castelo-Branco, M. (2021). Effects of anodal multichannel transcranial direct current stimulation (tDCS) on social-cognitive performance in healthy subjects: A randomized sham-controlled crossover pilot study. In *Progress in Brain Research* (Vol. 264, pp. 259–286). Elsevier B.V. https://doi.org/10.1016/bs.pbr.2021.04.004

Perin, C., Vigano, B., Piscitelli, D., Matteo, B. M., Meroni, R., & Cerri, C. G. (2020). Non-invasive current stimulation in vision recovery: A review of the literature. *Restorative Neurology and Neuroscience*, *38*(3), 239–250. https://doi.org/10.3233/RNN-190948

Potok, W., Post, A., Beliaeva, V., Bächinger, M., Cassarà, A. M., Neufeld, E., Polania, R., Kiper, D., & Wenderoth, N. (2023). Modulation of Visual Contrast Sensitivity with tRNS across the Visual System, Evidence from Stimulation and Simulation. *ENeuro*, *10*(6). https://doi.org/10.1523/ENEURO.0177-22.2023

Purves, D., Augustine, G. J., Fitzpatrick, D., Hall, W. C., LaMantia, A., & White, L. E. (2018). Neuroscience. New York Oxford University Press.

Reckow, J., Rahman-Filipiak, A., Garcia, S., Schlaefflin, S., Calhoun, O., DaSilva, A. F., Bikson, M., & Hampstead, B. M. (2018). Tolerability and blinding of 4x1 high-definition transcranial direct current stimulation (HD-tDCS) at two and three milliamps. *Brain Stimulation*, *11*(5), 991–997. https://doi.org/10.1016/j.brs.2018.04.022

Reinhart, R. M. G., Xiao, W., McClenahan, L. J., & Woodman, G. F. (2016). Electrical Stimulation of Visual Cortex Can Immediately Improve Spatial Vision. *Current Biology*, *26*(14), 1867–1872. https://doi.org/10.1016/j.cub.2016.05.019

Richard, B., Johnson, A. P., Thompson, B., & Hansen, B. C. (2015). The effects of tDCS across the spatial frequencies and orientations that comprise the contrast sensitivity function. *Frontiers in Psychology*, *6*(NOV). https://doi.org/10.3389/fpsyg.2015.01784

Rosa, A. M., Silva, M. F., Ferreira, S., Murta, J., & Castelo-Branco, M. (2013). Plasticity in the human visual cortex: An ophthalmology-based perspective. In *BioMed Research International* (Vol. 2013). Hindawi Limited. https://doi.org/10.1155/2013/568354

Sale, A., Berardi, N., Spolidoro, M., Baroncelli, L., & Maffei, L. (2010). GABAergic inhibition in visual cortical plasticity. *Frontiers in Cellular Neuroscience*, *4*(MAR). https://doi.org/10.3389/fncel.2010.00010

Sanches, C., Stengel, C., Godard, J., Mertz, J., Teichmann, M., Migliaccio, R., & Valero-Cabré, A. (2021). Past, Present, and Future of Non-invasive Brain Stimulation Approaches to Treat Cognitive Impairment in Neurodegenerative Diseases: Time for a Comprehensive Critical Review. In *Frontiers in Aging Neuroscience* (Vol. 12). Frontiers Media S.A. https://doi.org/10.3389/fnagi.2020.578339

Spiegel, D. P., Byblow, W. D., Hess, R. F., & Thompson, B. (2013). Anodal transcranial direct current stimulation transiently improves contrast sensitivity and normalizes visual cortex activation in individuals with amblyopia. *Neurorehabilitation and Neural Repair*, *27*(8), 760–769. https://doi.org/10.1177/1545968313491006

Spiegel, D. P., Li, J., Hess, R. F., Byblow, W. D., Deng, D., Yu, M., & Thompson, B. (2013). Transcranial Direct Current Stimulation Enhances Recovery of Stereopsis in Adults With

Amblyopia. *Neurotherapeutics*, *10*(4), 831–839. https://doi.org/10.1007/s13311-013-0200-y

Stagg, C. J., Best, J. G., Stephenson, M. C., O'Shea, J., Wylezinska, M., Kineses, Z. T., Morris, P. G., Matthews, P. M., & Johansen-Berg, H. (2009). Polarity-sensitive modulation of cortical neurotransmitters by transcranial stimulation. *Journal of Neuroscience*, *29*(16), 5202–5206. https://doi.org/10.1523/JNEUROSCI.4432-08.2009

Stagg, C. J., & Nitsche, M. A. (2011). Physiological basis of transcranial direct current stimulation. In *Neuroscientist* (Vol. 17, Issue 1, pp. 37–53). https://doi.org/10.1177/1073858410386614

Strang, C. E., Ray, M. K., Boggiano, M. M., & Amthor, F. R. (2018). Effects of tDCS-like electrical stimulation on retinal ganglion cells. *Eye and Brain*, *10*, 65–78. https://doi.org/10.2147/EB.S163914

Thompson, D. A., Bach, M., McAnany, J. J., Šuštar Habjan, M., Viswanathan, S., & Robson, A. G. (2024). ISCEV standard for clinical pattern electroretinography (2024 update). *Documenta Ophthalmologica*, *148*(2), 75–85. https://doi.org/10.1007/s10633-024-09970-1

Villamar, M. F., Volz, M. S., Bikson, M., Datta, A., Dasilva, A. F., & Fregni, F. (2013). Technique and considerations in the use of 4x1 ring high-definition transcranial direct current stimulation (HD-tDCS). *Journal of Visualized Experiments : JoVE*, *77*. https://doi.org/10.3791/50309

Wu, D., Li, C., Liu, N., Xu, P., & Xiao, W. (2020). Visual motion perception improvements following direct current stimulation over V5 are dependent on initial performance. *Experimental Brain Research*, *238*(10), 2409–2416. https://doi.org/10.1007/s00221-020-05842-7

Wu, D., Zhou, Y. J., Lv, H., Liu, N., & Zhang, P. (2021). The initial visual performance modulates the effects of anodal transcranial direct current stimulation over the primary visual cortex on the contrast sensitivity function. *Neuropsychologia*, *156*. https://doi.org/10.1016/j.neuropsychologia.2021.107854

Yamada, Y., & Sumiyoshi, T. (2021). Neurobiological Mechanisms of Transcranial Direct Current Stimulation for Psychiatric Disorders; Neurophysiological, Chemical, and Anatomical Considerations. In *Frontiers in Human Neuroscience* (Vol. 15). Frontiers Media S.A. https://doi.org/10.3389/fnhum.2021.631838

Zito, G. A., Senti, T., Cazzoli, D., Müri, R. M., Mosimann, U. P., Nyffeler, T., & Nef, T. (2015). Cathodal HD-tDCS on the right V5 improves motion perception in humans. *Frontiers in Behavioral Neuroscience*, *9*(September). https://doi.org/10.3389/fnbeh.2015.00257

High-definition transcranial direct current stimulation over the primary visual cortex in healthy adults: a multimodal visual and cortical approach

Rúben João Moreira da Cunha Magalhães

FACULDADE DE **MEDICINA**